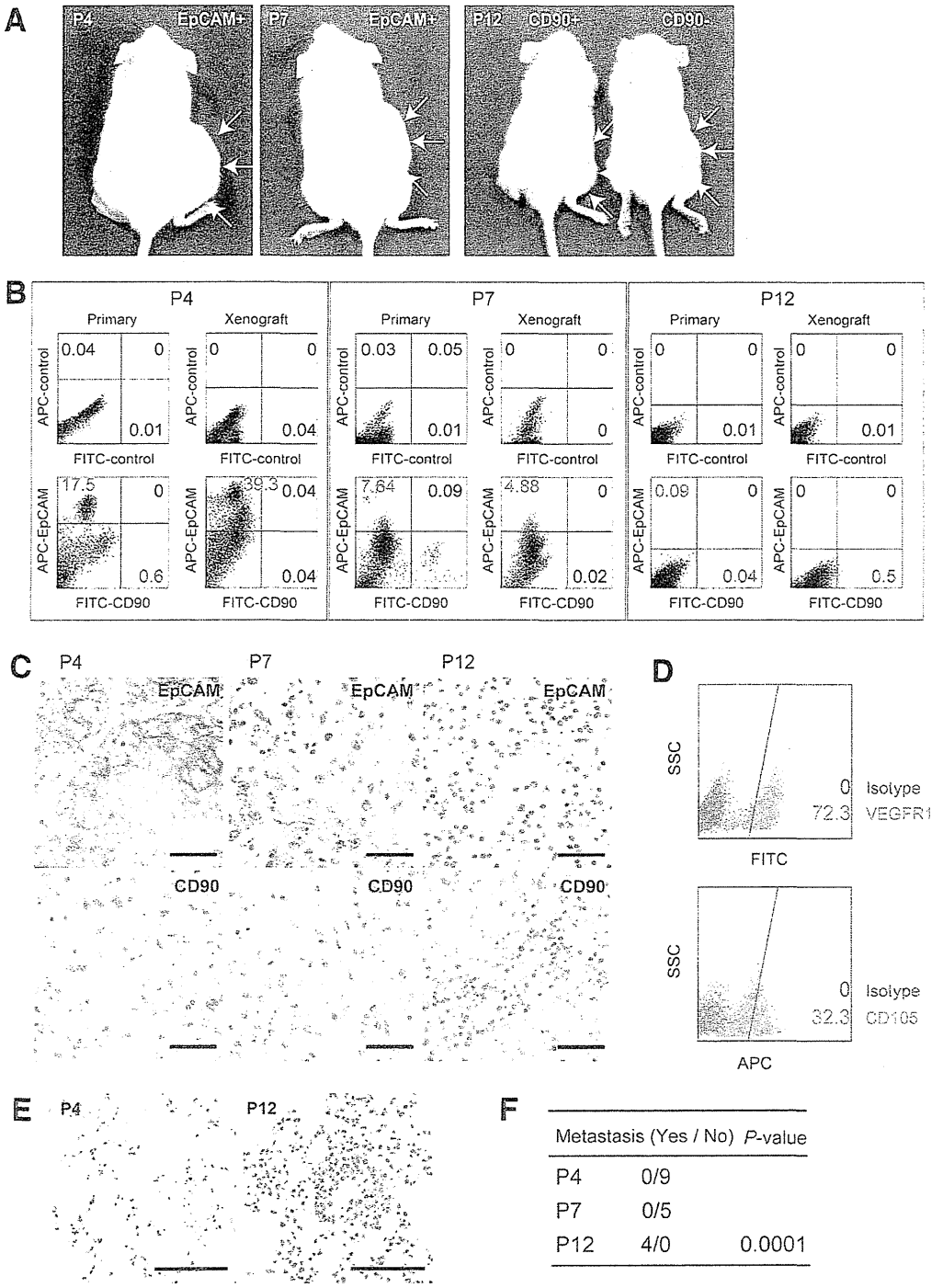


Fig. 5. Tumorigenic/metastatic capacities of EpCAM$^+$ and CD90$^+$ cells in primary HCC. (A) Representative NOD/SCID mice with SC tumors (white arrows) from EpCAM$^+$ P4 or P7 cells (left and middle panels) and CD90$^+$ or CD90$^-$ P12 cells (right panel). (B) FACS analysis of CD90 and EpCAM staining in primary HCCs and the corresponding secondary tumors developed in NOD/SCID mice. Unsorted cells ($1 \times 10^6$ cells in P4 and P7 or $1 \times 10^5$ cells in P12) were SC injected to evaluate the frequency of each marker-positive cell in primary and secondary tumors. (C) IHC analysis of EpCAM and CD90 in primary HCCs P4, P7, and P12 (scale bar, 50 $\mu$m). (D) FACS analysis of VEGFR1 (Alexa488) and CD105 (APC) in primary HCC P12. (E) Hematoxylin and eosin staining of lung tissues in P4 and P12 (scale bar, 200 $\mu$m). (F) Frequency of lung metastasis in NOD/SCID mice SC transplanted using unsorted primary HCC cells.

$\mu$M reduced cell proliferation and spheroid formation in CD90$^+$ cell lines, but had no effect on EpCAM$^+$ cell lines (Supporting Fig. S4B,C).

We further explored the effect of imatinib mesylate *in vivo*. Because EpCAM$^+$ and CD90$^+$ cells reside in the primary HCC, but not in established cell lines, we SC injected HuH7 and HLF cell lines to generate tumors organized by EpCAM$^+$ and CD90$^+$ CSCs. Interestingly, when HLF cells were coinjected with HuH7 cells, EpCAM$^+$ cells could metastasize to the lung, whereas

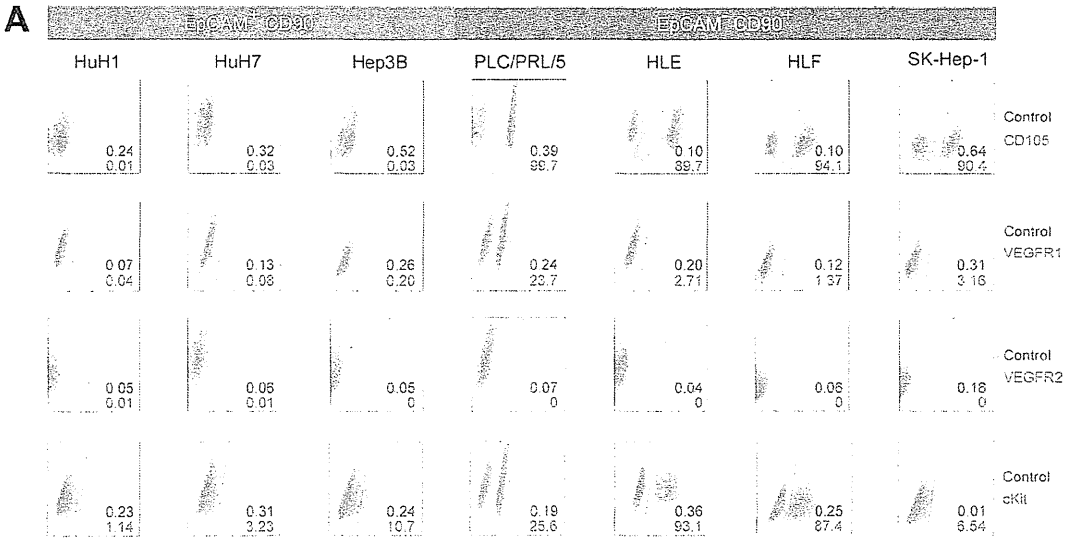


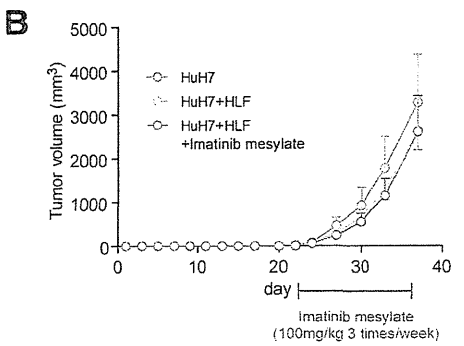


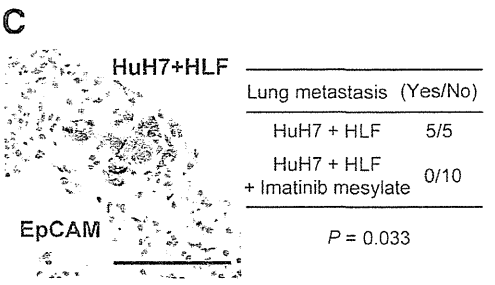


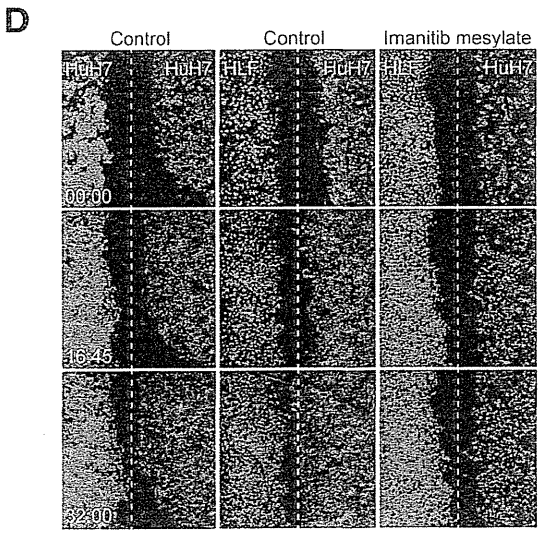


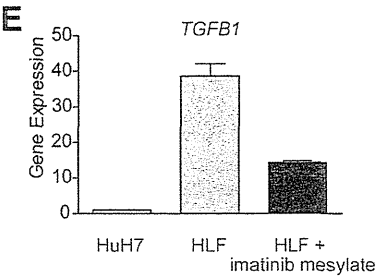


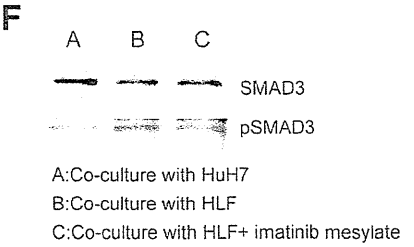

SC primary tumors showed no difference in size (Fig. 6B,C). Furthermore, although imatinib mesylate treatment had little effect on the size of primary SC tumors, it significantly suppressed lung metastasis in primary tumors (Fig. 6C). These data suggest that $CD90^+$ cells are not only metastatic to the distant organ, but also help the metastasis of $CD90^-$ cells, including $EpCAM^+$ cells, which originally have no distant metastatic capacity. Our data further suggest that imatinib mesylate can inhibit distant organ metastasis by suppressing $CD90^+$ metastatic CSCs, albeit with little effect on $EpCAM^+$ tumorigenic epithelial stem-like CSCs.

To explore the potential mechanism of how $CD90^+$ cells dictate the metastasis of $EpCAM^+$ cells, we utilized coculture systems and time-lapse image analysis. Wound-healing analysis clearly indicated that motility of HuH7 cells was enhanced when HLF cells were cocultured, and this effect was abolished by imatinib mesylate treatment (Fig. 6D; see Supporting Videos 1-3). HLF cells abundantly expressed *TGFB1*, compared with HuH7 cells, and its expression was dramatically suppressed by imatinib mesylate treatment (Fig. 6E). Mothers against decapentaplegic homolog 3 (Smad3) phosphorylation was augmented in HuH7 cells when cocultured with HLF cells, and this effect was attenuated when cocultured with HLF cells pretreated with imatinib mesylate.

Taken together, our data suggest that liver CSCs are not a single entity. Liver CSCs defined by different markers show unique features of tumorigenicity/metastasis with phenotypes closely associated with committed liver lineages. These distinct CSCs may collaborate to enhance tumorigenicity and metastasis of HCCs.

## Discussion

The current investigation demonstrates that CSC marker expression status may be a key determinant of cancer phenotypes, in terms of metastatic propensity and chemosensitivity, to certain molecularly targeted therapies. EpCAM appears to be an epithelial tumorigenic CSC marker, whereas CD90 seems to be a mesenchymal metastatic CSC marker associated with expression of c-Kit and chemosensitivity to imatinib mesylate. Imatinib mesylate may be effective in inhibiting metastasis, but has little effect on primary $EpCAM^+$ HCC cell growth.

We investigated the frequency of three CSC markers (EpCAM, CD90, and CD133) in 15 primary HCCs with a confirmed cell viability of $\geq$70% and found that three HCCs contained $CD133^+$ cells, seven HCCs contained $EpCAM^+$ cells, and all HCCs contained $CD90^+$ cells. Among them, we confirmed the perpetuation of $CD133^+$ cells derived from three HCCs (P7, P12, and P14; data not shown), $EpCAM^+$ cells derived from four HCCs (P4, P7, P13, and P14), and $CD90^+$ cells derived from two HCCs (P12 and P15). Recent studies showed that at least 8 of 21 HCCs (38%)[4] and 13 of 13 HCCs (100%)[5] contained tumorigenic $CD133^+$ or $CD90^+$ CSCs, respectively. Recent IHC and tissue microarray studies also demonstrated that $CD133^+$ and $CD90^+$ cells were detected in 24.8% ($\geq$1% of tumor cells) and 32.2% ($\geq$5% of tumor cells) of HCC cases examined, respectively.[15,16]

One possible explanation of the comparatively low frequency of $CD133^+$ liver CSCs identified in our study is that we used the monoclonal Ab CD133/2, whereas Ma et al. used CD133/1. Another possible explanation is the difference of etiology related to hepatocarcinogenesis. We examined tumorigenicity using 15 HCCs (five HBV related, four HCV related, three non-B, non-C hepatitis [NBNC] related, and three alcohol related) and identified that tumorigenic CSCs were only obtained from HBV- or HCV-related cases. Previous liver CSC studies were performed using HBV-related HCCs,[4,5] and a recent study showed that

Fig. 6. Suppression of lung metastasis mediated by $CD90^+$ CSCs by imatinib mesylate. (A) FACS analysis of seven HCC cell lines stained by APC-CD105, Alexa 488/VEGFR1, APC/VEGFR2, and Alexa 488/c-Kit Abs or isotype control. (B) Tumorigenicity of $5 \times 10^5$ HuH7 cells and $2.5 \times 10^5$ HuH7 cells plus $2.5 \times 10^5$ HLF cells treated with imatinib mesylate or control phosphate-buffered saline (PBS) (200 $\mu$L/mouse) orally ingested three times per week (100 mg/kg) for 2 weeks. Data are generated from 5 mice per condition. (C) IHC analysis of EpCAM in lung metastasis detected in NOD/SCID mice SC injected with $2.5 \times 10^5$ HuH7 cells and $2.5 \times 10^5$ HLF cells. Metastasis was evaluated macro- and microscopically in the left and right lobes of the lung separately in each mouse ($n = 5$) (scale bar, 100 $\mu$m). (D) Cell motility of HuH7 cells cocultured with HuH7, HLF, or HLF cells with imatinib mesylate (10 $\mu$M) was monitored in a real-time manner by time-lapse image analysis. HuH7 and HLF cells were labeled with the lipophilic fluorescence tracer, DiI (indicated as red) or DiD (indicated as blue), and incubated in a $\mu$-Slide eight-well chamber overnight. Silicone inserts were detached and the culture media replaced with Dulbecco's modified Eagle's medium containing 10% fetal bovine serum, including 0.1% dimethyl sulfoxide (DMSO) (control) or 10 $\mu$M of imatinib mesylate dissolved in DMSO (final concentration 0.1%). Immediately after the medium change, cells were cultured at 37°C in 5% $CO_2$ and time-lapse images were captured for 72 hours. (E) qPCR analysis of *TGFB1* in HuH7 (white bar), HLF (gray bar), and HLF cells pretreated with imatinib mesylate for 24 hours. (F) Smad3 and its phosphorylation evaluated by western blotting. HuH7 cells and HLF cells were harvested in cell culture inserts and treated with DMSO (0.1%) or imatinib mesylate (10 $\mu$M) for 24 hours. Cell culture inserts were washed with PBS, cocultured with HuH7 cells for 8 hours, and then removed. HuH7 cells were lysed using radioimmunoprecipitation assay buffer for western blotting. (A) HuH7 cells cocultured with HuH7 cells. (B) HuH7 cells cocultured with HLF cells. (C) HuH7 cells cocultured with HLF cells pretreated with imatinib mesylate.

HBV X may play a role in generating $EpCAM^+$ CSCs.[17] The role of hepatitis virus infection on the generation of CSCs is still unclear and should be clarified in future studies.

We were unable to confirm the tumorigenicity of $CD90^+$ cells in 13 of 15 HCCs, but we observed abundant $CD90^+$ cells in more-advanced HCCs by IHC (data not shown). Tumorigenic $CD90^+$ cells may emerge at a later stage of hepatocarcinogenesis, and the majority of $CD90^+$ cells in early HCCs may be cancer-associated VECs without tumorigenic capacity. Furthermore, we identified tumorigenic $CD90^+$ cells only from HBV-related HCCs, and a recent study suggested that expression of CD90 was associated with HBV infection.[16] We could not detect the small population of $CD90^+$ HuH7 and Hep3B cells reported on by Yang et al. However, because we identified a small population of $CD90^+$ HuH7 cells after treatment with 5-FU (manuscript in preparation), it is conceivable that different cellular stress statuses may explain the observed differences between our findings and those of Yang et al.

The majority of CSC markers discovered thus far are almost identical to those found in healthy tissue stem cells or embryonic stem cells. However, with regard to the liver, the characteristics of healthy hepatic stem/progenitor cells isolated using different stem cell markers are currently under investigation. A recent article examined the characteristics of $EpCAM^+$ and $CD90^+$ oval cells isolated from 2-acetylaminofluorene/partial hepatectomy or D-galactosamine-treated rats.[18] Interestingly, $EpCAM^+$ and $CD90^+$ oval cells represent two distinct populations: The former expresses classical oval cell markers, such as AFP, OV-1, and cytokeratin-19 (CK-19), whereas the latter expresses desmin and alpha smooth muscle actin, but not AFP, OV-1, or CK-19, which indicates that $CD90^+$ populations are more likely to be mesenchymal cells. Another study has demonstrated that mesenchymal cells can interact with HSCs to regulate cell-fate decision.[19] We found that $EpCAM^+$ and $CD90^+$ cells isolated from liver cancer are distinct in terms of gene- and protein-expression patterns in both primary liver cancers and cell lines. Furthermore, these distinct CSCs can interact to regulate the tumorigenicity and metastasis of HCC. Molecular characteristics of $EpCAM^+/CD90^+$ CSCs may potentially reflect the cellular context of healthy stem or progenitor cells.

Although our study strongly indicates that abundant $CD90^+$ cells in a tumor is a risk for distant metastasis in liver cancer, the cell identity and role of $CD90^+$ cells remains elusive. As our IHC, FACS, and xeno-transplantation assays revealed, some $CD90^+$ cells in liver cancer may be cancer-associated VECs or fibroblasts that cannot perpetuate in the xenograft. Recent findings have suggested the importance of stromal cells in tumorigenesis and cancer metastasis,[20-22] so it is possible that these cells may help TECs invade and intravasate into blood vessels, thus playing crucial roles in metastasis.

Another possibility is that $CD90^+$ cells are cancer cells with features of fibroblasts (having undergone EMT) or VECs (having undergone vasculogenic mimicry; VM) that can invade, intravasate, and metastasize cells to distant organs. Recently, two groups reported that a subset of tumor VECs originate from glioblastoma CSCs.[23,24] We successfully confirmed the tumorigenicity and metastatic capacity of $CD90^+$ cells that were morphologically identical to VECs from primary HCCs that could perpetuate in the xenograft. However, a recent study demonstrated that $CD90^+$ HCC cells express glypican-3, a marker detected in hepatic epithelial cells.[25] Further studies are warranted to clarify the nature and role of $CD90^+$ HCC cells.

In our study, $CD90^+$ cells expressed the endothelial marker, c-Kit, CD105, and VEGFR1, and a mesenchymal VEC morphology and high metastatic capacity were confirmed in both primary liver cancer and cell lines. We further confirmed that $CD90^+$ liver cancer cells showed chemosensitivity to imatinib mesylate, suggesting that cancer cells committed to mesenchymal endothelial lineages could be eradicated by the compound. Although imatinib mesylate treatment had little effect on the size of primary tumors originated from both $EpCAM^+$ and $CD90^+$ CSCs, it significantly suppressed lung metastasis *in vivo*. These data are consistent with a recent phase II study demonstrating the tolerable toxicity, but limited efficacy, of imatinib mesylate alone for unresectable HCC patients. Eligibility of imatinib mesylate for advanced HCC patients may be restricted to the HCC subtypes organized by $CD90^+$ CSCs with a highly metastatic capacity and VEC features. Therefore, a combination of compounds targeting $EpCAM^+$ tumorigenic CSCs as well as $CD90^+$ metastatic CSCs may be required for the eradication of HCC and should be tested in the future.

*Acknowledgments:* The authors thank Ms. Nami Nishiyama and Ms. Mikiko Nakamura for their excellent technical assistance.

## References

1. Tsai WL, Chung RT. Viral hepatocarcinogenesis. Oncogene 2010;29: 2309-2324.

2. Chiba T, Kita K, Zheng YW, Yokosuka O, Saisho H, Iwama A, et al. Side population purified from hepatocellular carcinoma cells harbors cancer stem cell-like properties. HEPATOLOGY 2006;44:240-251.
3. Haraguchi N, Ishii H, Mimori K, Tanaka F, Ohkuma M, Kim HM, et al. CD13 is a therapeutic target in human liver cancer stem cells. J Clin Invest 2010;120:3326-3339.
4. Ma S, Tang KH, Chan YP, Lee TK, Kwan PS, Castilho A, et al. miR-130b promotes CD133(+) liver tumor-initiating cell growth and self-renewal via tumor protein 53-induced nuclear protein 1. Cell Stem Cell 2010;7:694-707.
5. Yang ZF, Ho DW, Ng MN, Lau CK, Yu WC, Ngai P, et al. Significance of CD90+ cancer stem cells in human liver cancer. Cancer Cell 2008;13:153-166.
6. Zen Y, Fujii T, Yoshikawa S, Takamura H, Tani T, Ohta T, Nakanuma Y. Histological and culture studies with respect to ABCG2 expression support the existence of a cancer cell hierarchy in human hepatocellular carcinoma. Am J Pathol 2007;170:1750-1762.
7. Lee TK, Castilho A, Cheung VC, Tang KH, Ma S, Ng IO. CD24(+) liver tumor-initiating cells drive self-renewal and tumor initiation through STAT3-mediated NANOG regulation. Cell Stem Cell 2011;9: 50-63.
8. Yamashita T, Budhu A, Forgues M, Wang XW. Activation of hepatic stem cell marker EpCAM by Wnt-beta-catenin signaling in hepatocellular carcinoma. Cancer Res 2007;67:10831-10839.
9. Yamashita T, Forgues M, Wang W, Kim JW, Ye Q, Jia H, et al. EpCAM and alpha-fetoprotein expression defines novel prognostic subtypes of hepatocellular carcinoma. Cancer Res 2008;68:1451-1461.
10. Yamashita T, Ji J, Budhu A, Forgues M, Yang W, Wang HY, et al. EpCAM-positive hepatocellular carcinoma cells are tumor-initiating cells with stem/progenitor cell features. Gastroenterology 2009;136: 1012-1024.
11. Ma S, Chan KW, Hu L, Lee TK, Wo JY, Ng IO, et al. Identification and characterization of tumorigenic liver cancer stem/progenitor cells. Gastroenterology 2007;132:2542-2556.
12. Heffelfinger SC, Hawkins HH, Barrish J, Taylor L, Darlington GJ. SK HEP-1: a human cell line of endothelial origin. In Vitro Cell Dev Biol 1992;28A:136-142.
13. Ishimoto T, Nagano O, Yae T, Tamada M, Motohara T, Oshima H, et al. CD44 variant regulates redox status in cancer cells by stabilizing the xCT subunit of system xc(-) and thereby promotes tumor growth. Cancer Cell 2011;19:387-400.
14. Ramadori G, Fuzesi L, Grabbe E, Pieler T, Armbrust T. Successful treatment of hepatocellular carcinoma with the tyrosine kinase inhibitor imatinib in a patient with liver cirrhosis. Anticancer Drugs 2004;15: 405-409.
15. Kim H, Choi GH, Na DC, Ahn EY, Kim GI, Lee JE, et al. Human hepatocellular carcinomas with "Stemness"-related marker expression: keratin 19 expression and a poor prognosis. HEPATOLOGY 2011;54: 1707-1717.
16. Lu JW, Chang JG, Yeh KT, Chen RM, Tsai JJ, Hu RM. Overexpression of Thy1/CD90 in human hepatocellular carcinoma is associated with HBV infection and poor prognosis. Acta Histochem 2011;113: 833-838.
17. Arzumanyan A, Friedman T, Ng IO, Clayton MM, Lian Z, Feitelson MA. Does the hepatitis B antigen HBx promote the appearance of liver cancer stem cells? Cancer Res 2011;71:3701-3708.
18. Yovchev MI, Grozdanov PN, Zhou H, Racherla H, Guha C, Dabeva MD. Identification of adult hepatic progenitor cells capable of repopulating injured rat liver. HEPATOLOGY 2008;47:636-647.
19. Wang Y, Yao HL, Cui CB, Wauthier E, Barbier C, Costello MJ, et al. Paracrine signals from mesenchymal cell populations govern the expansion and differentiation of human hepatic stem cells to adult liver fates. HEPATOLOGY 2010;52:1443-1454.
20. Dome B, Timar J, Ladanyi A, Paku S, Renyi-Vamos F, Klepetko W, et al. Circulating endothelial cells, bone marrow-derived endothelial progenitor cells and proangiogenic hematopoietic cells in cancer: from biology to therapy. Crit Rev Oncol Hematol 2009;69:108-124.
21. Karnoub AE, Dash AB, Vo AP, Sullivan A, Brooks MW, Bell GW, et al. Mesenchymal stem cells within tumour stroma promote breast cancer metastasis. Nature 2007;449:557-563.
22. Mishra PJ, Humeniuk R, Medina DJ, Alexe G, Mesirov JP, Ganesan S, et al. Carcinoma-associated fibroblast-like differentiation of human mesenchymal stem cells. Cancer Res 2008;68:4331-4339.
23. Ricci-Vitiani L, Pallini R, Biffoni M, Todaro M, Invernici G, Cenci T, et al. Tumour vascularization via endothelial differentiation of glioblastoma stem-like cells. Nature 2010;468:824-828.
24. Wang R, Chadalavada K, Wilshire J, Kowalik U, Hovinga KE, Geber A, et al. Glioblastoma stem-like cells give rise to tumour endothelium. Nature 2010;468:829-833.
25. Ho DW, Yang ZF, Yi K, Lam CT, Ng MN, Yu WC, et al. Gene expression profiling of liver cancer stem cells by RNA-sequencing. PLoS One 2012;7:e37159.

Cancer Gene Therapy (2012) **19,** 312–319

www.nature.com/cgt

**ORIGINAL ARTICLE**

# Membrane-bound form of monocyte chemoattractant protein-1 enhances antitumor effects of suicide gene therapy in a model of hepatocellular carcinoma

Y Marukawa[1], Y Nakamoto[1], K Kakinoki[1], T Tsuchiyama[1], N Iida[1], T Kagaya[1], Y Sakai[1], M Naito[2], N Mukaida[3] and S Kaneko[1]

Suicide gene therapy using the herpes simplex virus thymidine kinase/ganciclovir (HSV-tk/GCV) system combined with monocyte chemoattractant protein-1 (MCP-1) provides significant antitumor efficacy. The current study was designed to evaluate the antitumor immunity of a newly developed membrane-bound form of MCP-1 (mMCP-1) in an immunocompetent mouse model of hepatocellular carcinoma (HCC). A recombinant adenovirus vector (rAd) harboring the human *MCP-1* gene and the membrane-spanning domain of the *CX3CL1* gene was used. Large amounts of MCP-1 protein were expressed and accumulated on the tumor cell surface. The growth of subcutaneous tumors was markedly suppressed when tumors were treated with mMCP-1, as compared with soluble MCP-1, in combination with the HSV-tk/GCV system ($P<0.01$). The numbers of Mac-1-, CD4- and CD8a-positive cells were significantly higher in tumor tissues ($P<0.05$), and tumor necrosis factor (TNF) mRNA expression levels with mMCP-1 were almost five-fold higher than those with soluble MCP-1. These results indicate that the delivery of the *mMCP-1* gene greatly enhanced antitumor effects following the apoptotic stimuli by promoting the recruitment and activation of macrophages and T lymphocytes, suggesting a novel strategy of immune-based gene therapy in the treatment of patients with HCC.

*Cancer Gene Therapy* (2012) **19,** 312–319; doi:10.1038/cgt.2012.3; published online 9 March 2012

**Keywords:** herpes simplex virus thymidine kinase; hepatocellular carcinoma; membrane-bound form; monocyte chemoattractant protein-1; monocyte/macrophages

## INTRODUCTION

In spite of the recent development of locoregional treatments for hepatocellular carcinoma (HCC), the frequency of tumor recurrence remains high, probably because of insufficient therapeutic effects and the multicentric development of HCC in cirrhotic liver.[1–3] Non-surgical treatments of HCC, such as radiofrequency ablation, transcatheter arterial embolization and transcatheter arterial chemotherapy induce apoptosis of HCC cells, but these treatments do not enhance antitumoral immunity sufficiently. Thus, gene therapy aimed at enhancing antitumor immune responses may be a promising approach to prevent HCC recurrence, when it is combined with non-surgical maneuvers.

We previously reported that monocyte chemoattractant protein-1 (*MCP-1*) gene delivery using recombinant adenovirus vector (rAd) *in vivo* can enhance the efficacy of suicide gene therapy consisting of the delivery of rAd containing herpes simplex virus thymidine kinase (HSV-tk) and ganciclovir (GCV) in models of HCC[4,5] and colon cancer.[6] We further demonstrated that the antitumor effects depended on the activation of macrophages.[4,5] The adenovirus-specific spatial and temporal expression pattern may result in the production of the transgene for a limited time.[7] Mirroring these characteristics, the adenovirus vector-mediated delivery of the *MCP-1* gene alone was not sufficient to reduce tumor growth.[5] To circumvent this bottleneck, sustained expression of MCP-1 at the tumor site may be required to enhance the efficacy of the gene therapy using the *MCP-1* gene.

Systemic or local administration of cytokines has been used to enhance the antitumor immune response induced by many cancer vaccines. However, the systemic administration of cytokines resulted in unwanted side effects. Recently, tumor therapy that uses a membrane-bound form of cytokine was developed to reduce the side effects of cytokine in the systemic circulation. These experiments revealed that the membrane-bound form of cytokine not only reduced the side -effects, but enhanced the antitumor effects by prolonging the half-life of cytokines in the tumor microenvironment.[8]

These observations prompted us to design the adenovirus vector driving the expression of membrane-bound form of MCP-1 (mMCP-1) and to evaluate its antitumor effects in a model of HCC. We demonstrated that the delivery of the *mMCP-1* gene markedly augmented HSV-tk/GCV suicide gene therapy, compared with that of the soluble MCP-1 (sMCP-1).

## MATERIALS AND METHODS

### Recombinant adenovirus vectors

Ad-mMCP-1 (Figure 1a) harboring the human *MCP-1* gene and the membrane-spanning domain of the *CX3CL1* gene driven by the human cytomegalovirus

[1]Department of Disease Control and Homeostasis, Graduate School of Medical Science, Kanazawa University, Kanazawa, Japan; [2]Division of Cellular and Molecular Pathology, Niigata University Graduate School of Medicine, Niigata, Japan and [3]Division of Molecular Bioregulation, Cancer Research Institute, Kanazawa University, Kanazawa, Japan. Correspondence: Dr S Kaneko, Department of Disease Control and Homeostasis, Graduate School of Medical Science, Kanazawa University, 13-1 Takara-machi, Kanazawa 920-8641, Japan.
E-mail: skaneko@m-kanazawa.jp
Received 5 July 2011; revised 5 December 2011; accepted 26 January 2012; published online 9 March 2012

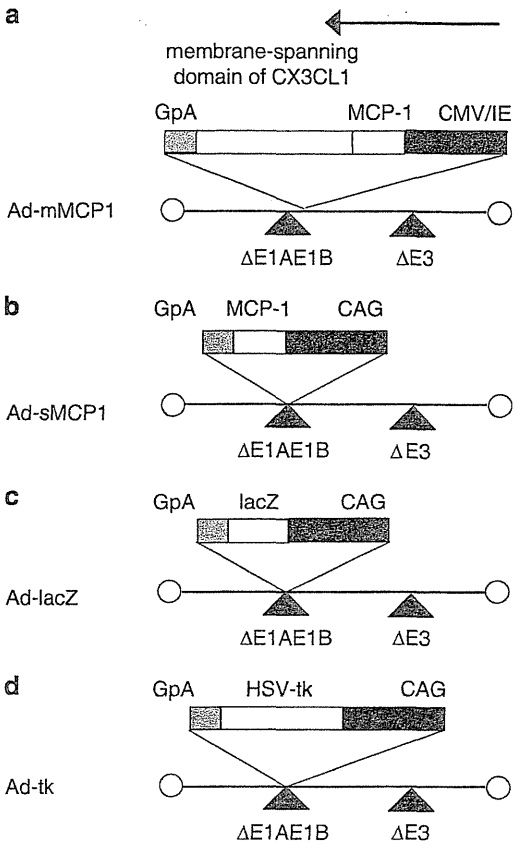


**Figure 1.** Construct of recombinant adenovirus vector (rAds). Under the control of the cytomegalovirus immediate early promoter/enhancer (CMV/IE) promoter and the CAG promoter, rAd Ad-membrane-bound monocyte chemoattractant protein-1 (mMCP-1) (**a**) expressing human MCP-1 and the membrane-spanning domain of fractalkine/CX3CL1 in sequence, rAd Ad-soluble-MCP-1 (sMCP-1), (**b**) expressing MCP-1, rAd Ad-lacZ, (**c**) expressing lacZ and rAd Ad-tk, (**d**) expressing HSV-tk. Solid lines indicate the rAd genome. An open triangle below the rAd genome represents a deletion of adenovirus early regions. Arrows show the orientations of the transcription. GpA, rabbit β-globin poly (A) site.

immediate early promoter/enhancer was prepared, purified and titrated according to the protocols supplied by the manufacturer (Takara, Tokyo, Japan). The human MCP-1/CX3CL1 (fractalkine) chimera was designed as follows: DNA encoding a fragment of human CX3CL1 spanning the intracellular, transmembrane and partial extracellular region was amplified from the full-length CX3CL1 cDNA by PCR with the following primers (5′-GCGAGCTCGGGTACCTTCGAGAAGCAGATCG-3′ and 5′-GCGAATTCAGATT GTCACACGGGCACAGG-3′). *Sac*I, *Kpn*I and *Eco*RI restriction enzyme sites were added at the 5′ and 3′ ends of this fragment. MCP-1 was also amplified by PCR with the following primers (5′-GCGAGCTCGCCAGCAT-GAAAGTCTCTGCCG-3′ and 5′-GCGGTACCAGTCTTCGGAGTTTGGGTTTGC-3′). *Sac*I and *Kpn*I restriction enzyme sites were added at the 5′ and 3′ ends of this fragment. The CX3CL1 and MCP-1 DNA fragments were digested with restriction enzymes by coligation into the *Sac*I and *Eco*RI sites of pSTBlue-1 (Novagen, Darmstadt, Germany), generating pSTBlue-1-mMCP-1. Then, pSTBlue-1-mMCP-1 was digested by *Not*I and *Bam*HI restriction enzymes and the fragment was inserted into the pShuttle Vector (Clontech Laboratories, Mountain View, CA) under the control of cytomegalovirus immediate early promoter/enhancer, generating pShuttle-mMCP-1. The pShuttle-mMCP-1 was digested with *PI-SceI/I-CeuI* (New England Biolabs, Hitchin, UK) and the purified product was ligated with Adeno-X genome DNA, containing nearly the full length of the adenovirus type 5 genome lacking the E1 and E3 regions, to generate pAd.mMCP-1. Subsequently, Ad-mMCP-1 was generated by transfecting 293 cells with pAd.mMCP-1, which was linearized with *Pac*I, as described in the manual. Ad-sMCP-1 (which expresses sMCP-1), Ad-lacZ (which expresses beta-galactosidase (lacZ)) and Ad-tk (which expresses HSV-tk) were constructed as previously described and propagated in 293 cells (Figures 1b-d).[9] The rAds were purified on a cesium gradient, and the titer of rAd was determined by the 50% tissue culture infectious dose ($TCID_{50}$) method.[10]

## Cell lines and culture

The mouse HCC cell lines (BNL 1NG A2, BNL 1ME A.7R. 1, MM45T.Li and Hepa 1-6) and the colon cancer cell line Colon 26 were used in these experiments. Cells were cultured in Dulbecco's modified Eagle medium (Gibco, Long Island, NY) supplemented with 10% heat-inactivated fetal bovine serum (Gibco).

## ELISA for MCP-1

Aliquots of $1 \times 10^5$ HCC lines (BNL 1NG A2, BNL 1ME A.7R. 1, MM45T.Li and Hepa 1-6) and the colon cancer cell line, Colon 26 clone 20, were seeded in 1.0 ml of culture media in a six-well tissue culture plate. After 24 h, the cells were infected with Ad-mMCP-1, Ad-sMCP-1 and Ad-lacZ at various multiplicities of infection (MOI). After 48 h, the cells were harvested and sonicated to obtain the membrane fractions, and the media was collected from each well. Tumor tissues were resected on day 1 after subcutaneous injection of $5 \times 10^6$ MM45T.Li cells infected with indicated rAds (MOI 50) as described below. Tumor tissues were washed with phosphate-buffered saline (PBS) and sonicated to obtain the membrane fractions. The concentration of MCP-1 was determined by enzyme-linked immunosorbent assay (ELISA) as described previously.[11] Briefly, each well of a 96-well microtiter plate was coated with monoclonal anti-human MCP-1 antibody (ME61; 1 mg $ml^{-1}$) overnight at 41 °C. After washing, the plates were blocked by incubation with PBS containing 1% bovine serum albumin for 1 h at 37 °C. Diluted sample media was added, and the plate was then incubated for 2 h at 37 °C. Following incubation, the plates were washed and incubated with rabbit anti-MCP-1 antibody (1 mg $ml^{-1}$), followed by alkaline phosphatase-conjugated goat anti-rabbit antibody (1/12 000, Tago, Burlingame, CA), each for 2 h at 37 °C. After the plate was washed, aliquots of 1 mg $ml^{-1}$ p-nitrophenylphosphate (Sigma, St Louis, MO) in 1 M diethanolamine (Sigma; pH 9.8) supplemented with 0.5 mM $MgCl_2$ were added to the wells, and the plate was incubated for 40 min at room temperature. After the addition of 1 M NaOH, the optical density (405 nm wavelength–OD405) was assessed by using an ELISA plate reader (MTP-120; Corona Electric, Ibaragi, Japan).

## *In vitro* chemotaxis assay

*In vitro* migration assays were performed with the QCM chemotaxis cell migration assay (5 μm, Chemicon International, Temecula, CA) according to the manufacturer's instructions. Briefly, $7.5 \times 10^4$ splenocytes were resuspended in 100 μl of RPMI1640 containing 5% bovine serum albumin, and loaded into the upper well of a transwell chamber. The lower wells were filled with 150 μl of supernatant from MM45T.Li cells that were harvested 48 h after infection with rAds. The cells were incubated for 4 h at 37 °C in a humidified, 5% $CO_2$ atmosphere. The migrated cells were lysed and detected by the CyQuant GR dye (Molecular Probes, Eugene, OR), and fluorescence was read at an excitation wavelength of 490 nm and an emission wavelength of 520 nm in a fluorescence microplate reader (Thermo Scientific Fluoroskan Ascent FL, Thermo Fisher Scientific Oy, Vantaa, Finland).

## *In vitro* proliferation assay

*In vitro* proliferation assays were performed with the CellTiter 96 Aqueous Non-Radioactive Cell Proliferation Assay (Promega, Madison, WI) according to the manufacturer's instructions. Briefly, aliquots of $1 \times 10^4$ MM45T.Li cells that were harvested 24 h after infection with rAds were seeded in a 96-well tissue culture plate and incubated for 24 h. MTS [3-(4,5-dimethylthiazol-2-yl)-5-(3-carboxymethoxyphenyl)-2-(4-sulfophenyl)-2H-tetrazolium] solution was added and incubated for 2 h, and the absorbance

at 490 nm was measured by using an ELISA plate reader (MTP-120; Corona Electric).

### Animal studies

The following investigations were performed in accordance with the guidelines of our Institutional Animal Care and Use Committee. Six-week-old immunocompetent female BALB/c-jcl mice (CLEA Japan, Tokyo, Japan) were injected subcutaneously on both sides of the flank on day 0 with $3 \times 10^5$ MM45T.Li cells infected with each rAd at an *in vitro* MOI of 5. For the next 5 days (days 1-5), mice received 75 mg $kg^{-1}$ of intraperitoneally administered GCV (Tanabe Pharmaceutical Drug, Tokyo, Japan). In some series of experiment, 1 μg of the recombinant human MCP-1 in 200 μl of PBS containing 1% bovine serum albumin were injected intraperitoneally, as previously described,[12] from days 0 to 2 (3 consecutive days) in the group of the tumor cells transduced with Ad-lacZ on HSV-tk/GCV suicide therapy. Tumor sizes were measured every 3 days, and tumor volumes were calculated according to the formula (longest diameter)/(shortest diameter)$^2$/2.

### Immunohistochemical analysis

Tumor tissues and spleens were resected on day 10. The tissue samples were embedded in OCT compound (Sakura Finetek, Toorrance, CA) and snap-frozen in liquid nitrogen. Cryostat sections of the frozen tissues were fixed with 4% paraformaldehyde in PBS, followed by washing once with distilled water for 5 min and three times with PBS for 5 min. To avoid nonspecific staining, avidin and biotin in the tissues were blocked by using a blocking kit (Vector Laboratories, Burlingame, CA).

The tissue sections were subsequently stained with rat anti-mouse CD4 Ab, rat anti-mouse CD8a Ab, rat anti-mouse CD11b Ab (BD Biosciences, San Diego, CA), or monoclonal mouse anti-human MCP-1 Ab (R&D systems, Minneapolis, MN) overnight at 4 °C. Isotype controls were also used. Then, the slides were incubated for 0.5 h at room temperature with biotinylated polyclonal rabbit anti-rat IgG (Dako Cytomation, Tokyo, Japan), or the antibodies in the M.O.M. immunodetection kit to detect mouse primary antibodies on mouse tissues (Vector Laboratories). The reactions were visualized by using a VectaStain ABC standard kit (Vector Laboratories), followed by counterstaining with hematoxylin. The positive cells were counted in 10 randomly chosen fields at 400-fold magnification by an examiner without any prior knowledge of the experimental procedures.

### Quantitative real-time reverse-transcriptase PCR

Total RNA was extracted from tumor tissues resected on day 10 using an RNeasy Mini kit (Qiagen, Hilden, Germany) according to the manufacturer's instructions. After treating the RNA preparations with ribonuclease-free DNase I (Qiagen) to remove residual DNA, cDNA was synthesized as described previously.[13] Quantitative real-time PCR was performed on a StepOne real-time PCR system (Applied Biosystems, Foster City, CA) by using the comparative $C_T$ quantification method. TaqMan Gene Expression Assays (Applied Biosystems) containing specific primers (assay ID: tumor necrosis factor (TNF), Mm00443258_m1; glyceraldehyde-3-phosphate dehydrogenase (GAPDH), Mm99999915_g1), TaqMan MGB probe (FAM dye-labeled), and TaqMan Fast Universal PCR Master Mix were used with 10 ng cDNA to quantify the expression levels of TNF. Reactions were performed for 20 s at 95 °C followed by 40 cycles of 1 s at 95 °C and 20 s at 60 °C. The GAPDH was amplified as an internal control, and the GAPDH $C_T$ values were subtracted from $C_T$ values of the target genes ($C_T$). The $\Delta C_T$ values of tumors after immune gene therapy with both the suicide gene (HSV-tk system) and rAds were compared respectively.

### Flow cytometry

MM45T.Li. cells transfected with rAds were resuspended in PBS containing 1% bovine serum albumin and 0.1% sodium azide and incubated for 30 min on ice with PE-conjugated rat anti-human MCP-1 (BD Pharmingen, San Diego, CA). The cells were washed, resuspended in PBS and analyzed in a FACScan with CellQuest software (FACSCalibur, BD Biosciences, San Jose, CA).

*Depletion of macrophages/monocytes.* Clodronate liposome was prepared and systemic depletion of monocytes/macrophages was performed as previously described.[14,15] Mice were intraperitoneally injected with 200 μl of clodronate liposome five times: days −2, 0, 3, 6 and 10 after tumor injection. PBS-clodronate was given in the same manner as a negative control. Depletion of CD11c-negative monocytes in blood was confirmed by flow cytometry after injection of clodronate liposome.

### Statistical analysis

Mean and s.d. or s.e. were calculated for the obtained data. The statistical significance of differences between groups was evaluated by the Mann-Whitney *U*-test. $P<0.05$ was considered statistically significant.

## RESULTS

### *In vitro* and *in vivo* MCP-1 production by cells infected with recombinant adenoviruses

When various tumor cells were infected with either Ad-mMCP-1 or Ad-sMCP-1 at an MOI of 10, the cells did not show any signs of cell death (data not shown). Both types of adenoviruses induced the secretion of human MCP-1 into the supernatants to similar levels in all the cell lines that we examined (Figure 2a). On the contrary, MCP-1 contents in the membrane fractions were higher in the cells infected with Ad-mMCP-1 than in those with Ad-sMCP-1 (Figure 2a). The proportion of MCP-1-positive cells were progressively augmented in MM45T.Li cells as the MOIs of the used Ad-mMCP-1 were increased (Figure 2b). In contract, MCP-1-positive cells were not detected in tumor cells infected with Ad-sMCP-1 and Ad-lacZ, even when the cells were infected with either vector at a MOI of 100 (Figure 2b). Thus, Ad-mMCP-1 infection can *in vitro* drive human MCP-1 expression on the cell surface, as well as its secretion into the culture medium. These results indicate that large amounts of MCP-1 protein were expressed and accumulated on the tumor cell surface when tumor cells were infected with Ad-mMCP-1 as compared with Ad-sMCP-1 *in vitro*. To define the biological functions of secreted human MCP-1 protein, we examined the migratory capacity of splenocytes to the culture supernatants obtained 24 h after the infection. The supernatants from either Ad-mMCP-1- or Ad-sMCP-1-infected cells enhanced the transmigration of splenic lymphocytes to similar extents, compared with those from Ad-lacZ-infected cells (Figure 2c). These results indicated that biologically active human MCP-1 was secreted into the culture supernatants.

### Proliferation of tumor cells infected with rAds *in vitro* and *in vivo*

To quantify the proliferation of tumor cells infected with rAds, the MTS assay was performed 24 h after infection. The optical absorbance at 490 nm of tumor cells did not change in the presence or absence of rAd infection (Figure 3a). Next, tumor cells infected with rAds (MOI 10) *ex vivo* were transferred subcutaneously in syngeneic wild-type mice, and tumor development was monitored (Figure 3b). Tumor cells infected with Ad-mMCP-1 and Ad-sMCP-1 showed similar growth rates to tumor cells infected with Ad-lacZ. These results indicate that infection with the rAds used in this study did not affect the proliferation of tumor cells *in vitro* and *in vivo*, and that the delivery of mMCP-1 did not display antitumor activity when used alone. In addition, the levels of MCP-1 expression were confirmed immunohistochemically in the subcutaneous tumor tissues (Figure 3c). MCP-1-positive tumor cells were detected in tumor tissues infected with Ad-mMCP-1; however, the cells were negative for MCP-1 staining in tissues infected with Ad-sMCP-1 and Ad-lacZ. Moreover, larger amounts of MCP-1 were detected in the tumor tissues of the mice treated with Ad-mMCP-1 than in those with Ad-sMCP-1 (Figure 3d). The data indicated that large amounts of MCP-1 protein were expressed and accumulated on the tumor cell surface when the tumor cells were infected with Ad-mMCP-1 *in vivo*.

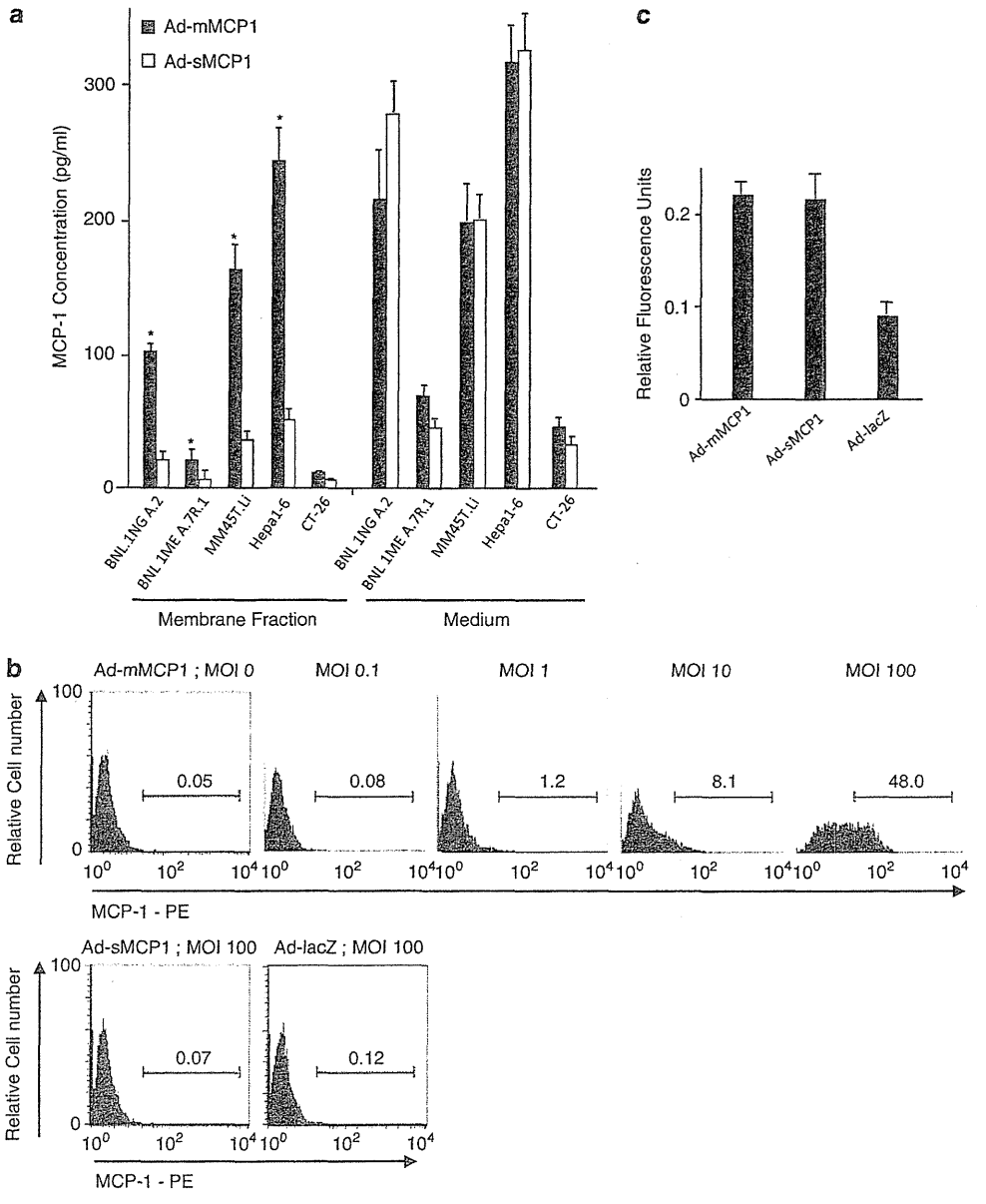


**Figure 2.** Monocyte chemoattractant protein-1 (MCP-1) production in tumor cells infected with recombinant adenovirus vectors (rAds). (**a**) Concentrations of MCP-1 in the membrane fractions and in the media of hepatoma cells (BNL 1NG A.2, BNL 1ME A.7R.1, MM45T.Li and Hepa1-6) and colon cancer cells (colon 26 clone 20) infected with rAds at multiplicities of infection (MOI) of 10 were measured by enzyme-linked immunosorbent assay (ELISA). Each value is the mean s.d. of triplicate experiments. *, $P<0.05$ when compared with Ad-soluble MCP-1 (sMCP-1) by the Mann–Whitney's *U*-test. (**b**) Surface expression of MCP-1 on MM45T.Li cells infected with rAds (Ad-mMCP-1, Ad-sMCP-1 and Ad-lacZ) at the indicated MOIs was assessed by flow cytometry by using PE-conjugated anti-human MCP-1 antibody. Histograms represent MCP-1 staining of tumor cells. Numbers indicate percentages of MCP-1-positive cells. Surface MCP-1-positive cells were detected in 0.08, 1.2, 8.1 and 48.0% of MM45T.Li cells infected by Ad-mMCP-1 at MOIs of 0.1, 1, 10 and 100, respectively. The results are representative of three independent experiments. (**c**) The migratory activity of MCP-1 secreted from rAd-infected tumor cells. Mouse splenic lymphocytes were loaded into the upper wells of transwell chambers, and supernatants of tumor cells infected with rAds at an MOI of 10 were added to the lower wells. Cells that migrated through the 8-μm pores to the feeder tray after 4 h incubation were lysed and detected by CyQuant GR dye that exhibits enhanced fluorescence upon binding cellular nucleic acids. Each value is the mean s.e. of data from three separate migration chambers.

### Potentiation of HSV-tk/GCV suicide therapy by co-infection with Ad-mMCP-1

We previously demonstrated that the gene delivery of Ad-sMCP-1 enhanced the antitumor effects of the HSV-tk/GCV system.[4-6,16,17] Hence, we compared the effects of Ad-mMCP-1 and Ad-sMCP-1 infection on HSV-tk/GCV suicide therapy. When MM45T.Li cells were co-infected with Ad-tk and Ad-lacZ, and received GCV, tumor growth was delayed marginally but not significantly (Figure 4a). Co-infection with Ad-tk and Ad-sMCP-1 retarded tumor growth significantly after GCV treatment. Moreover, tumor growth was almost abrogated by the combination of co-infection with Ad-tk and Ad-mMCP-1, and GCV treatment. To address whether the antitumor effects could be induced not only by the gene delivery using Ad vector, but also by the administration of recombinant protein, we gave intraperitoneally recombinant MCP-1 to the animals, which were injected with tumor cells, treated with

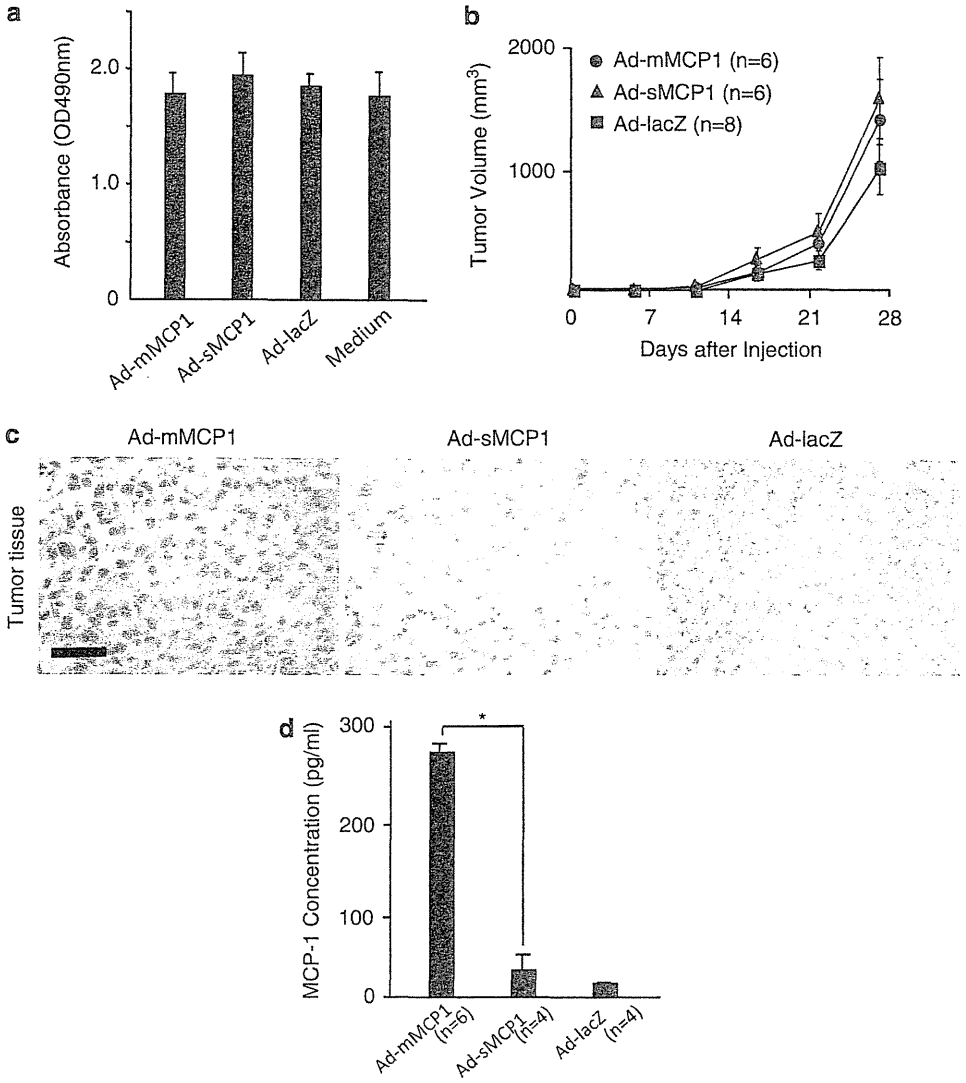


**Figure 3.** Proliferation of tumor cells infected with recombinant adenovirus vectors (rAds) *in vitro* and *in vivo*. (**a**) Tumor cell growth after the infection of indicated rAds *in vitro*. A total of $5 \times 10^5$ of MM45T.Li cells were infected with the rAds at multiplicities of infection (MOI) of 10 and incubated for 24 h. The cell numbers were quantitated by MTS (3-(4,5-dimethylthiazol-2-yl)-5-(3-carboxymethoxyphenyl)-2-(4-sulfophenyl)-2H-tetrazolium) assay. The absorbance was determined at 490 nm with a microplate reader. Each value is the mean s.d. of data from triplicate experiments. (**b**) Tumor cell growth after infection of indicated rAds in mice. BALB/c mice were subcutaneously injected with $3 \times 10^5$ MM45T.Li cells infected with the rAds at an MOI of 10 on day 0. Tumor diameters were monitored. Each value is the mean s.e. (**c**) Immunohistochemical analysis of subcutaneous tumor tissues 7 days after the injection in panel **b**. Tissues were stained and visualized by using anti-human monocyte chemoattractant protein-1 (MCP-1) Ab and ABC methods. MCP-1 expression was seen as brown in the cytoplasm of tumor cells. The bar represents 30 μm. Original magnification, ×400. (**d**) Concentrations of MCP-1 were measured in the s.c. tumor tissues resected on day 1 after injection of $5 \times 10^6$ MM45T.Li cells infected with the indicated rAds at an MOI of 50 by enzyme-linked immunosorbent assay (ELISA). Each value is the mean s.d. of duplicate experiments. $^*P < 0.05$ when compared with Ad-sMCP-1 by the Mann-Whitney's *U*-test.

Ad-lacZ and Ad-tk. The systemic administration of recombinant MCP-1 rather enhanced tumor growth (Figure 4b). As we previously demonstrated that MCP-1 can promote tumor growth in a context-dependent manner by recruiting macrophages, which can secrete an angiogenic factor, the vascular endothelial growth factor,[16,18] systemic MCP-1 injection may promote tumor growth by its pro-angiogenic activities.

### Recruitment and activation of macrophages and T lymphocytes in tumor tissues

The GCV treatment following co-infection with Ad-lacZ and Ad-tk failed to increase the intratumoral numbers of Mac-1-positive macrophages, CD4-positive lymphocytes and CD8-positve lymphocytes, compared with GCV treatment following Ad-lacZ infection (Figures 5A and B). GCV administration following co-infection with Ad-sMCP-1 and Ad-tk increased the intratumoral Mac-1-positive macrophage, CD4-positive lymphocyte and CD8-positve lymphocyte numbers (Figure 5A and B). The increases were further enhanced by GCV treatment following co-infection with Ad-mMCP-1 and Ad-tk (Figures 5A and B). Moreover, intratumoral mRNA expression of TNF, a known macrophage and T lymphocyte secretagogue, was markedly enhanced in tumors co-infected with Ad-mMCP-1, compared with those with Ad-sMCP-1 plus Ad-tk. To evaluate the functional contribution of intratumoral immune cells, we depleted CD11c-negative

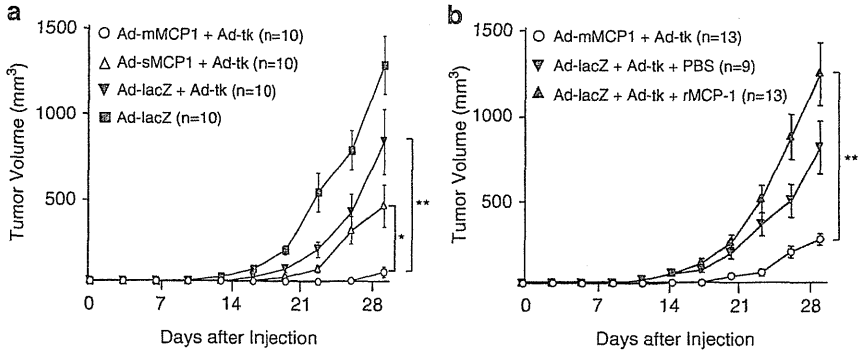


**Figure 4.** Antitumor effects of recombinant adenovirus vector (rAds) *in vivo*. (**a**) BALB/c mice were subcutaneously injected with $3 \times 10^5$ MM45T.Li cells infected with rAds Ad-membrane-bound monocyte chemoattractant protein-1 (mMCP-1) + Ad-tk, Ad-soluble MCP-1 (sMCP-1) + Ad-tk, Ad-lacZ + Ad-tk, and Ad-lacZ at multiplicities of infection (MOI) of 10 on day 0. Subsequently, 75 mg $kg^{-1}$ of ganciclovir (GCV) was administered for 5 consecutive days (days 2–6). Each value is the mean s.e. of triplicate experiments. *$P<0.05$ when compared with Ad-sMCP-1 + Ad-tk, and **$P<0.01$ when compared with Ad-lacZ + Ad-tk by the Mann–Whitney's *U*-test. (**b**) BALB/c mice were injected with MM45T.Li cells and treated as described in the legend to (**a**). In Ad-lacZ + Ad-tk + recombinant human MCP-1 (rMCP-1) group, the mice were injected with 1 μg of rMCP-1 intraperitoneally from days 0 to 2 (3 consecutive days). The mice were injected with phosphate-buffered saline (PBS) as controls. Tumor sizes were measured every 3 days. Each value is the mean s.e. **$P<0.01$ when compared with Ad-lacZ + Ad-tk + rMCP-1 by the Mann–Whitney's *U*-test.

monocytes/macrophages by intraperitoneal administration of clodronate liposome in the current mouse model. The monocyte/macrophage-depleted mice developed larger tumor than those treated with PBS liposome (Figure 5D), indicating that monocytes/macrophages were critically involved in the suppression of tumor growth by Ad-mMCP-1. Collectively, these data demonstrate that the delivery of mMCP-1 promoted the recruitment and activation of macrophages and T lymphocytes in tumor tissues, presumably leading to the beneficial antitumor responses in this model.

## DISCUSSION

We have proposed a strategy for improving the efficacy of suicide gene-based gene therapy by the combined heterochronic administration of *HSV-tk* and *MCP-1* genes.[4-6,16-18] In the current study, we generated recombinant adenovirus Ad-mMCP-1 expressing a fusion protein containing the human MCP-1 cDNA fused with the membrane-spanning domain of fractalkine/CX3CL1, to drive more efficient and sessile expression of MCP-1. Ad-mMCP-1 infection did not affect the proliferation of MM45T.Li tumor cells *in vitro* or *in vivo*, by itself. Of interest is that Ad-mMCP-1 infection pontentiated HSV-tk/GCV suicide therapy more efficiently than Ad-sMCP-1. Moreover, Ad-mMCP-1-mediated antitumor effects were associated with the recruitment and activation of macrophages and T lymphocytes in tumor tissues. Collectively, the delivery of membrane-bound *MCP-1* gene can augment antitumor effects caused by the HSV-tk/GCV system in an immunecompetent mouse model of liver tumor and therefore, can be a novel strategy of immune-based gene therapy to prevent tumor proliferation and recurrence in patients with HCC.

Chimeric membrane-bound cytokine gene expression vectors were generated to drive the efficient expression on tumor cell surface and to reduce the severe side effects caused by systemic administration of high doses of cytokines. With this maneuver, cytokines can be anchored on the cell plasma membrane. As a consequence, a locally high concentration of cytokines can be achieved with ease and their *in vivo* half-life can be prolonged in the tumor site. The availability of cytokines on tumor cell surface can eventually bring immune cells to the tumor site for better antigen uptake and stimulation, thereby inducing antitumor effects at a higher efficiency. On the basis of these assumptions, this type of modified cytokine gene therapy has been reported on interleukin-2,[13,19,20] interleukin-12,[21] fractalkine (CX3CL1)[22] and TNF.[23] Indeed, accumulating evidence revealed that the membrane-bound form of cytokine genes can exhibit more antitumor effects than the corresponding soluble ones. Likewise, the current study confirms that the membrane-bound form of MCP-1 can attract more immune cells, including monocytes/macrophages and T lymphocytes, to the tumor sites and can induce the expression of TNF. In addition, TNF can activate endothelial cells to express several adhesion molecules, such as the intercellular adhesion molecules and vascular cell adhesion molecules.[24-27] Circulating immune cells can utilize these adhesion molecules to effectively transmigrate into the tissues in addition to the direct chemotactic activities exerted by MCP-1.

The effects of MCP-1 on tumor growth was controversial, either destructive[28-30] or protective[31,32] in a context-dependent manner. Likewise, murine colon carcinoma cell expressing MCP-1 failed to metastasize when injected into mice,[28] whereas other carcinoma cells showed enhanced metastasis.[31] These discrepancies may be explained by the observations reported by Nesbit *et al.*[33] They demonstrated that low-level MCP-1 secretion with modest monocyte infiltration resulted in tumor formation, whereas high secretion was associated with massive monocyte/macrophage infiltration into the tumor mass, leading to its destruction within a few days. Thus, systemic MCP-1 administration may not be able to induce massive monocyte/macrophage infiltration into tumor mass and may promote tumor mass as we observed in the present study. Moreover, we previously revealed that suicide therapy can induce tumor cell apoptosis and that apoptotic tumor cells can secrete MCP-1 more efficiently, thereby recruiting a massive number of macrophages and retarding tumor growth.[4] Consistently, we further demonstrated that the delivery of an optimal amount of rAd expressing MCP-1 enhanced the antitumor effects of the HSV-tk/GCV system in a model of HCC.[16,18] Infection with Ad-mMCP-1 can sustain MCP-1 expression in tumor tissues more efficiently than that with Ad-sMCP-1 as evidenced by an immunohistochemical analysis on the infected tumor tissues. The sustained MCP-1 expression can potentiate suicide gene therapy more efficiently.

The present data suggest that the use of Ad-mMCP-1 can be promising, but several problems remain to be solved before the clinical application. First, subcutaneous tumor models of an HCC cell line may not be relevant to HCCs in patients. However, in cases of nonsurgical procedures for HCC treatment in patients, such as percutaneous radiofrequency ablation therapy[34] and

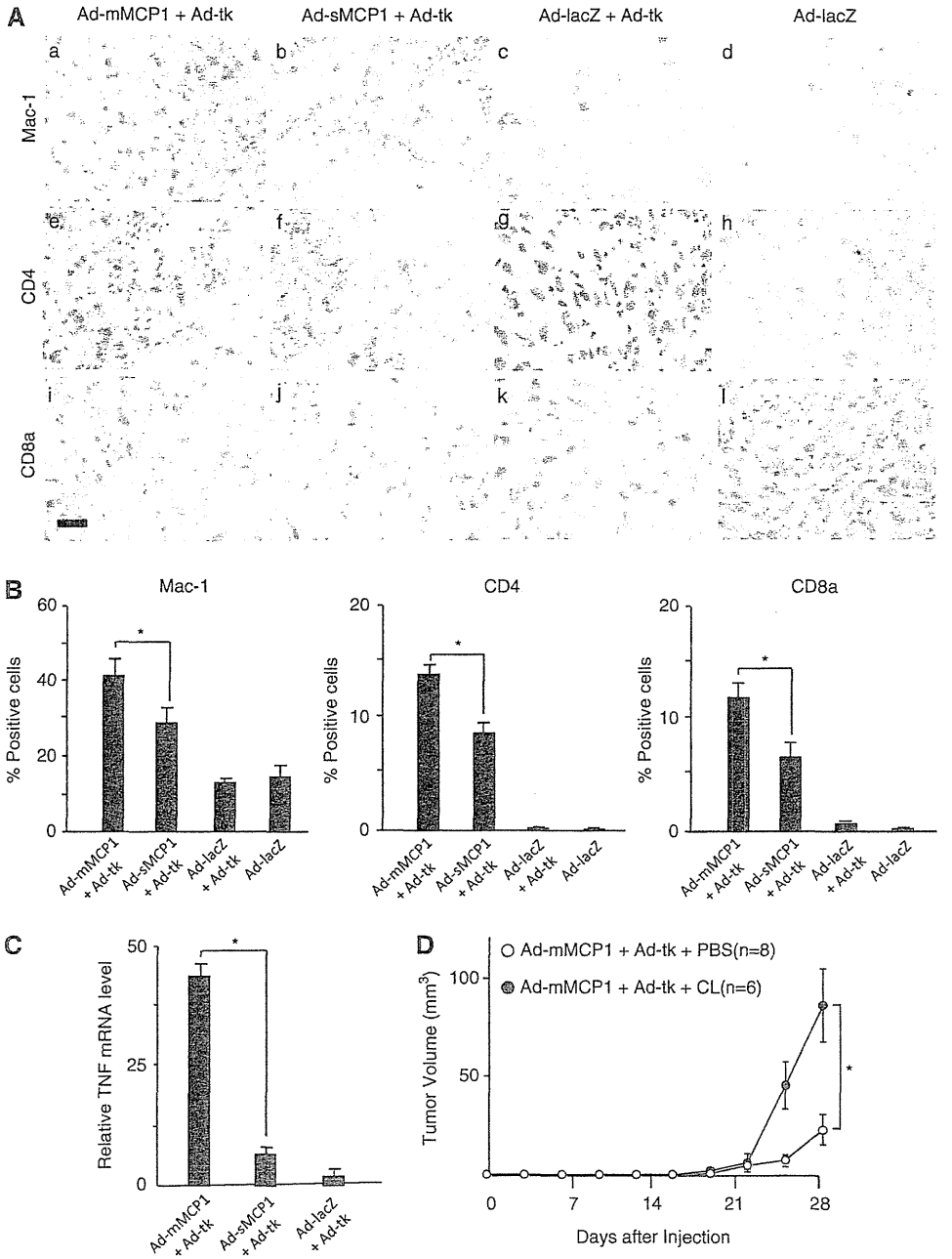


**Figure 5.** Immunohistochemical analysis for Mac-1-, CD4- and CD8a-positive cells and expression of tumor necrosis factor (TNF) mRNA in tumor tissues. In the experiment described in the legend to Figure 4, tumors were resected on day 10 and used for the analyses. (**A**) Tumor tissues treated with Ad-membrane-bound monocyte chemoattractant protein-1 (mMCP-1) + Ad-tk (a, e and i), Ad-soluble MCP-1 (sMCP-1) + Ad-tk (b, f and j), Ad-lacZ + Ad-tk (c, g and k) and Ad-lacZ (d, h and l) were stained with anti-Mac-1 antibody (a–d), anti-CD4 antibody (e–h) or anti-CD8a antibody (i–l). Positive cells are seen as brown. Original magnification, × 400. (**B**) Quantitative morphometric analysis showing the proportions of positive cells in areas of 100 tumor cells. Ten high-power ( × 400) fields of tumor tissue were examined. Results are expressed as means per 1000 hepatoma cells. Values are the means s.d. of triplicate experiments. *$P<0.05$ when compared with Ad-sMCP-1 by the Mann–Whitney's *U*-test. (**C**) Real-time PCR analysis for TNF mRNA expression in tumor tissues, presented relative to glyceraldehyde 3-phosphate dehydrogenase (GAPDH) mRNA. Each value is the mean s.d. of duplicate experiments. *$P<0.05$ when compared with Ad-sMCP-1 + Ad-tk by the Mann–Whitney *U*-test. (**D**) BALB/c mice were subcutaneously injected with MM45T.Li cells infected with indicated rAds and treated as described in the legend to Figure 4a. In the Ad-mMCP-1 + Ad-tk + clodronate liposome (CL) group, mice were injected with 200 μl of CL to deplete monocytes/macrophages as described in Materials and methods. The mice were injected with phosphate-buffered saline (PBS) liposome as controls. Tumor sizes were measured every 3 days. Each value is the mean s.e. *$P<0.05$ when compared with Ad-mMCP-1 + Ad-tk + PBS by the Mann–Whitney's *U*-test.

transcatheter arterial chemotherapy,[35] administration of the current rAd vectors could be easily applied, immediately once the standard nonsurgical procedures to ensure tumor cell killing. Moreover, rAd can elicit its immunogenicity or cytotoxicity when administered in HCC patients, particularly by the use of intraarterial procedures. Actually, the infection of high doses of rAds causes severe unexpected side effects.[36] However, the delivery of membrane-bound form of the *MCP-1* gene can cause

a high and effective concentration at the tumor sites even when it is administered at a relatively lower titer, and therefore, can evade severe adverse effects caused frequently by the administration of a high titer of adenovirus vectors.

## CONFLICT OF INTEREST

The authors declare no conflict of interest.

## ACKNOWLEDGEMENTS

We thank Mariko Katsuda for assistance with histopathological analysis and immunohistochemistry, and Maki Kawamura and Chiharu Minami for providing animal care.

## REFERENCES

1 Venook AP. Treatment of hepatocellular carcinoma: too many options? *J Clin Oncol* 1994; **12**: 1323-1334.
2 Trinchet JC, Beaugrand M. Treatment of hepatocellular carcinoma in patients with cirrhosis. *J Hepatol* 1997; **27**: 756-765.
3 Bruix J. Treatment of hepatocellular carcinoma. *Hepatology* 1997; **25**: 259-262.
4 Sakai Y, Kaneko S, Nakamoto Y, Kagaya T, Mukaida N, Kobayashi K. Enhanced antitumor effects of herpes simplex virus thymidine kinase/ganciclovir system by codelivering monocyte chemoattractant protein-1 in hepatocellular carcinoma. *Cancer Gene Ther* 2001; **8**: 695-704.
5 Tsuchiyama T, Kaneko S, Nakamoto Y, Sakai Y, Honda M, Mukaida N *et al.* Enhanced antitumor effects of a bicistronic adenovirus vector expressing both herpes simplex virus thymidine kinase and monocyte chemoattractant protein-1 against hepatocellular carcinoma. *Cancer Gene Ther* 2003; **10**: 260-269.
6 Kagaya T, Nakamoto Y, Sakai Y, Tsuchiyama T, Yagita H, Mukaida N *et al.* Monocyte chemoattractant protein-1 gene delivery enhances antitumor effects of herpes simplex virus thymidine kinase/ganciclovir system in a model of colon cancer. *Cancer Gene Ther* 2006; **13**: 357-366.
7 Freund CT, Sutton MA, Dang T, Contant CF, Rowley D, Lerner SP. Adenovirus-mediated combination suicide and cytokine gene therapy for bladder cancer. *Anticancer Res* 2000; **20**: 1359-1365.
8 Kim YS. Tumor therapy applying membrane-bound form of cytokines. *Immune Netw* 2009; **9**: 158-168.
9 Sato Y, Tanaka K, Lee G, Kanegae Y, Sakai Y, Kaneko S *et al.* Enhanced and specific gene expression via tissue-specific production of Cre recombinase using adenovirus vector. *Biochem Biophys Res Commun* 1998; **244**: 455-462.
10 Kanegae Y, Makimura M, Saito I. A simple and efficient method for purification of infectious recombinant adenovirus. *Jpn J Med Sci Biol* 1994; **47**: 157-166.
11 Ko Y, Mukaida N, Panyutich A, Voitenok NN, Matsushima K, Kawai T *et al.* A sensitive enzyme-linked immunosorbent assay for human interleukin-8. *J Immunol Methods* 1992; **149**: 227-235.
12 Nakano Y, Kasahara T, Mukaida N, Ko YC, Nakano M, Matsushima K. Protection against lethal bacterial infection in mice by monocyte-chemotactic and -activating factor. *Infect Immun* 1994; **62**: 377-383.
13 Ji J, Li J, Holmes LM, Burgin KE, Yu X, Wagner TE *et al.* Glycoinositol phospholipid-anchored interleukin 2 but not secreted interleukin 2 inhibits melanoma tumor growth in mice. *Mol Cancer Ther* 2002; **1**: 1019-1024.
14 Lu P, Li L, Liu G, van Rooijen N, Mukaida N, Zhang X. Opposite roles of CCR2 and CX3CR1 macrophages in alkali-induced corneal neovascularization. *Cornea* 2009; **28**: 562-569.
15 Sadahira Y, Yasuda T, Yoshino T, Manabe T, Takeishi T, Kobayashi Y *et al.* Impaired splenic erythropoiesis in phlebotomized mice injected with CL2MDP-liposome: an experimental model for studying the role of stromal macrophages in erythropoiesis. *J Leukoc Biol* 2000; **68**: 464-470.
16 Tsuchiyama T, Nakamoto Y, Sakai Y, Mukaida N, Kaneko S. Optimal amount of monocyte chemoattractant protein-1 enhances antitumor effects of suicide gene therapy against hepatocellular carcinoma by M1 macrophage activation. *Cancer Sci* 2008; **99**: 2075-2082.
17 Tsuchiyama T, Nakamoto Y, Sakai Y, Marukawa Y, Kitahara M, Mukaida N *et al.* Prolonged, NK cell-mediated antitumor effects of suicide gene therapy combined with monocyte chemoattractant protein-1 against hepatocellular carcinoma. *J Immunol* 2007; **178**: 574-583.
18 Kakinoki K, Nakamoto Y, Kagaya T, Tsuchiyama T, Sakai Y, Nakahama T *et al.* Prevention of intrahepatic metastasis of liver cancer by suicide gene therapy and chemokine ligand 2/monocyte chemoattractant protein-1 delivery in mice. *J Gene Med* 2010; **12**: 1002-1013.
19 Chang MR, Lee WH, Choi JW, Park SO, Paik SG, Kim YS. Antitumor immunity induced by tumor cells engineered to express a membrane-bound form of IL-2. *Exp Mol Med* 2005; **37**: 240-249.
20 Ji J, Li J, Holmes LM, Burgin KE, Yu X, Wagner TE *et al.* Synergistic anti-tumor effect of glycosylphosphatidylinositol-anchored IL-2 and IL-12. *J Gene Med* 2004; **6**: 777-785.
21 Nagarajan S, Selvaraj P. Glycolipid-anchored IL-12 expressed on tumor cell surface induces antitumor immune response. *Cancer Res* 2002; **62**: 2869-2874.
22 Tang L, Hu HD, Hu P, Lan YH, Peng ML, Chen M *et al.* Gene therapy with CX3CL1/Fractalkine induces antitumor immunity to regress effectively mouse hepatocellular carcinoma. *Gene Ther* 2007; **14**: 1226-1234.
23 Rieger R, Whitacre D, Cantwell MJ, Prussak C, Kipps TJ. Chimeric form of tumor necrosis factor-alpha has enhanced surface expression and antitumor activity. *Cancer Gene Ther* 2009; **16**: 53-64.
24 Nooijen PT, Eggermont AM, Verbeek MM, Schalkwijk L, Buurman WA, de Waal RM *et al.* Transient induction of E-selectin expression following TNF alpha-based isolated limb perfusion in melanoma and sarcoma patients is not tumor specific. *J Immunother Emphasis Tumor Immunol* 1996; **19**: 33-44.
25 Yang L, Froio RM, Sciuto TE, Dvorak AM, Alon R, Luscinskas FW. ICAM-1 regulates neutrophil adhesion and transcellular migration of TNF-alpha-activated vascular endothelium under flow. *Blood* 2005; **106**: 584-592.
26 Vanhee D, Delneste Y, Lassalle P, Gosset P, Joseph M, Tonnel AB. Modulation of endothelial cell adhesion molecule expression in a situation of chronic inflammatory stimulation. *Cell Immunol* 1994; **155**: 446-456.
27 VandenBerg E, Reid MD, Edwards JD, Davis HW. The role of the cytoskeleton in cellular adhesion molecule expression in tumor necrosis factor-stimulated endothelial cells. *J Cell Biochem* 2004; **91**: 926-937.
28 Huang S, Singh RK, Xie K, Gutman M, Berry KK, Bucana CD *et al.* Expression of the JE/MCP-1 gene suppresses metastatic potential in murine colon carcinoma cells. *Cancer Immunol Immunother* 1994; **39**: 231-238.
29 Rollins BJ, Sunday ME. Suppression of tumor formation *in vivo* by expression of the JE gene in malignant cells. *Mol Cell Biol* 1991; **11**: 3125-3131.
30 Nokihara H, Yanagawa H, Nishioka Y, Yano S, Mukaida N, Matsushima K *et al.* Natural killer cell-dependent suppression of systemic spread of human lung adenocarcinoma cells by monocyte chemoattractant protein-1 gene transfection in severe combined immunodeficient mice. *Cancer Res* 2000; **60**: 7002-7007.
31 Nakashima E, Mukaida N, Kubota Y, Kuno K, Yasumoto K, Ichimura F *et al.* Human MCAF gene transfer enhances the metastatic capacity of a mouse cachectic adenocarcinoma cell line *in vivo*. *Pharm Res* 1995; **12**: 1598-1604.
32 Ueno T, Toi M, Saji H, Muta M, Bando H, Kuroi K *et al.* Significance of macrophage chemoattractant protein-1 in macrophage recruitment, angiogenesis, and survival in human breast cancer. *Clin Cancer Res* 2000; **6**: 3282-3289.
33 Nesbit M, Schaider H, Miller TH, Herlyn M. Low-level monocyte chemoattractant protein-1 stimulation of monocytes leads to tumor formation in nontumorigenic melanoma cells. *J Immunol* 2001; **166**: 6483-6490.
34 Curley SA. Radiofrequency ablation of malignant liver tumors. *Ann Surg Oncol* 2003; **10**: 338-347.
35 Tung-Ping Poon R, Fan ST, Wong J. Risk factors, prevention, and management of postoperative recurrence after resection of hepatocellular carcinoma. *Ann Surg* 2000; **232**: 10-24.
36 Marshall E. Gene therapy death prompts review of adenovirus vector. *Science* 1999; **286**: 2244-2245.

# TNF-α and Tumor Lysate Promote the Maturation of Dendritic Cells for Immunotherapy for Advanced Malignant Bone and Soft Tissue Tumors

**Shinji Miwa[1], Hideji Nishida[1], Yoshikazu Tanzawa[1], Munetomo Takata[1], Akihiko Takeuchi[1], Norio Yamamoto[1], Toshiharu Shirai[1], Katsuhiro Hayashi[1], Hiroaki Kimura[1], Kentaro Igarashi[1], Eishiro Mizukoshi[2], Yasunari Nakamoto[2], Shuichi Kaneko[2], Hiroyuki Tsuchiya[1]***

**1** Department of Orthopaedic Surgery, Kanazawa University School of Medicine, Kanazawa, Japan, **2** Department of Disease Control and Homeostasis, Kanazawa University School of Medicine, Kanazawa, Japan

## Abstract

*Background:* Dendritic cells (DCs) play a pivotal role in the immune system. There are many reports concerning DC-based immunotherapy. The differentiation and maturation of DCs is a critical part of DC-based immunotherapy. We investigated the differentiation and maturation of DCs in response to various stimuli.

*Methods:* Thirty-one patients with malignant bone and soft tissue tumors were enrolled in this study. All the patients had metastatic tumors and/or recurrent tumors. Peripheral blood mononuclear cells (PBMCs) were suspended in media containing interleukin-4 (IL-4) and granulocyte-macrophage colony stimulating factor (GM-CSF). These cells were then treated with or without 1) tumor lysate (TL), 2) TL + TNF-α, 3) OK-432. The generated DCs were mixed and injected in the inguinal or axillary region. Treatment courses were performed every week and repeated 6 times. A portion of the cells were analyzed by flow cytometry to determine the degree of differentiation and maturation of the DCs. Serum IFN-γ and serum IL-12 were measured in order to determine the immune response following the DC-based immunotherapy.

*Results:* Approximately 50% of PBMCs differentiated into DCs. Maturation of the lysate-pulsed DCs was slightly increased. Maturation of the TL/TNF-α-pulsed DCs was increased, commensurate with OK-432-pulsed DCs. Serum IFN-γ and serum IL-12 showed significant elevation at one and three months after DC-based immunotherapy.

*Conclusions:* Although TL-pulsed DCs exhibit tumor specific immunity, TL-pulsed cells showed low levels of maturation. Conversely, the TL/TNF-α-pulsed DCs showed remarkable maturation. The combination of IL-4/GM-CSF/TL/TNF-α resulted in the greatest differentiation and maturation for DC-based immunotherapy for patients with bone and soft tissue tumors.

**Citation:** Miwa S, Nishida H, Tanzawa Y, Takata M, Takeuchi A, et al. (2012) TNF-α and Tumor Lysate Promote the Maturation of Dendritic Cells for Immunotherapy for Advanced Malignant Bone and Soft Tissue Tumors. PLoS ONE 7(12): e52926. doi:10.1371/journal.pone.0052926

**Editor:** Isaac Yang, UCLA, United States of America

**Received** May 14, 2012; **Accepted** November 22, 2012; **Published** December 21, 2012



**Funding:** The authors have no support or funding to report.

**Competing Interests:** The authors have declared that no competing interests exist.

* E-mail: tsuchi@med.kanazawa-u.ac.jp

## Introduction

Dendritic cells (DCs) play a pivotal role in the immune system, bridging the innate and adaptive immune responses [1–3]. DCs are critical professional antigen-presenting cells (APCs), crucially important in the capture, processing and presenting of tumor antigens to tumor-specific T cells [4,5]. Necrotic tumor debris contains endogenous "danger signals", required for the activation and maturation of APCs. DCs reach the damaged tissue, take up tumor antigens in the context of inflammation and abundant cytokines, and undergo a change in phenotype characterized by the upregulation of cell surface markers, such as costimulatory, adhesion and integrin molecules. The activated APCs migrate to tumor-draining lymph nodes where they present tumor antigens on major histocompatibility complex (MHC) molecules, as well as costimulatory signals, to resting tumor-specific T cells, inducing their activation [6]. Activated effector $CD4^+$ T cells can attack MHC class $II^+$ tumors and provide help to a variety of antitumor effector cells, including $CD8^+$ cytotoxic T cells, B cells and macrophages [7–9].

There are a number of experimental and clinical studies about DC-based immunotherapies [10–12]. In the study of malignant bone and soft tissue tumors, there are some reports concerning DC-based immunity. Joyama reported that DCs inhibit primary tumors and metastatic tumors in an osteosarcoma model using LM8 [13]. Kawano reported that frozen tumor and DCs inhibit metastatic tumors, and increase IFN-γ and the migration of CD8-positive cells to the metastatic site in the osteosarcoma model [14]. These reports suggest that DC-based immunotherapy may be effective in the treatment of sarcoma. However, there are few reports about DC-based immunotherapy for malignant bone and soft tissue tumor.

DCs are present in peripheral blood. However, the concentration of DCs in the blood cells is too low to make their collection

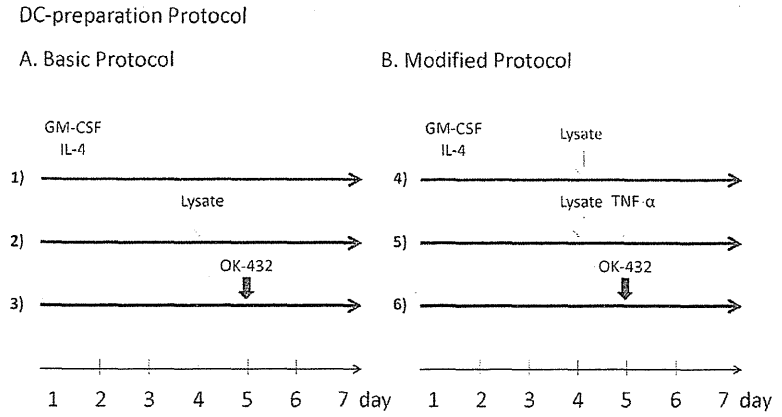


**Figure 1. Preparation of DC from peripheral blood monocytes. A. Basic DC-preparation Protocol.** DCs were generated from peripheral blood (50 ml) collected from study patients. Mononuclear cells were isolated by density gradient centrifugation on Lymphoprep. Interphase cells were removed, washed twice in phosphate-buffered saline (PBS), and suspended in CellGro. After adherence for 2 hours, adherent cells were cultured in media containing IL-4 (50 ng/ml) and GM-CSF (100 ng/ml). On days 4 and 5, the cultures were additionally supplemented with or without tumor lysate (TL) (100 μg/ml) and OK-432 (0.1 KE/ml). **B. Modified DC-preparation Protocol.** TNF-α was added to the protocol of tumor lysate and OK432. Similar to the first DC preparation protocol, the cells were cultured in a medium containing IL-4 and GM-CSF. On days 4 and 5, the cultures were additionally supplemented with or without tumor lysate (TL) (100 μg/ml), rhTNF-α (100 ng/ml), and OK-432 (0.1 KE/ml).
doi:10.1371/journal.pone.0052926.g001

practical for clinical applications [15]. Instead, DCs are manufactured in either hematopoietic stem cells or peripheral blood monocytes [15,16]. DCs are most frequently produced from peripheral blood mononuclear cells (PBMCs). Immature DCs are generated from PBMCs by suspension in media containing interleukin-4 (IL-4) and granulocyte-macrophage colony stimulating factor (GM-CSF) for several days. In the steady state, nonactivated (immature) DCs present self-antigens to T cells, which leads to tolerance [17,18]. Conversely, activated (mature) DCs initiate antigen-specific immunity, resulting in T-cell proliferation and differentiation into helper and effector cells. DCs are also important in launching humoral immunity, partly because of their capacity to directly interact with B cells and to present unprocessed antigens. Therefore, the maturation of DCs is important for DC-based immunotherapy. Immature DCs (iDC) can be matured using various exogenous stimuli, including cytokines, growth factors, costimulatory molecules and inflammatory signals. Although various methods of generating DCs have been reported, the methods for differentiation and maturation of DCs are controversial. In this study, we developed methods for DC maturation using tumor necrotic factor alpha (TNF-α). The aim of our study was to generate and to investigate the differentiation and maturation of DCs. DCs were generated using various stimuli on PBMCs from patients with advanced malignant bone and soft tissue tumors.

## Patients and Methods

### Patients

Inclusion criteria were as follows: radiological and pathological diagnosis of malignant bone and soft tissue tumor, surgically resected tumor, age ≥6 years old, informed consent, and performance status (PS) ≤2.

Exclusion criteria included: severe cardiac, renal, pulmonary, hematological or other systemic disease associated with a discontinuation risk; chemotherapy or radiation therapy within four weeks; immunological disorders including splenectomy and radiation of the spleen; corticosteroid or anti-histamine therapy; or difficulty in follow-up.

This study protocol was approved by the Institutional Review Board of the Kanazawa University Graduate School of Medical Science, Kanazawa, Japan. This study complied with ethical standards outlined in the Declaration of Helsinki. Written informed consent was obtained from all patients and/or their parents before entry of the patients into this study. In cases that the patients were under twenty years old, the informed consent was obtained from all the parents.

### Preparation of Tumor Lysates

Tumor lysates (TL) were prepared from tumor tissues obtained from resected tumors. A portion of the tumor tissues (1 $cm^3$) was frozen in liquid nitrogen for 20 min, and then thawed at room temperature for 20 min. The freeze-thaw cycle was repeated two times. Then, the tumor tissues were stirred and centrifuged, and supernatants were collected through a 0.2 μm filter. The amounts of protein in TL were evaluated by protein assay using a Bio-Rad protein assay kit (Bio-Rad, Tokyo, Japan) and stored at −20°C for later use.

### Preparation of Autologous Dendritic Cells (DCs)

As previously reported, DCs were generated from blood monocyte precursors [19,20]. Briefly, PBMCs from each patients were isolated by centrifugation in LymphoprepTM Tubes (Nycomed, Roskilde, Denmark). For generating DCs, PBMCs were plated in six-well tissue culture dishes (Costar, Cambridge, MA, USA) at 1– $4\times10^7$ cells in 2 ml per well and allowed to adhere to plastic for 2 h. Adherent cells were cultured in serum-free media (GMP CellGro® DC Medium; CellGro, Manassas, VA, USA) with 50 ng/ml recombinant human IL-4 (GMP grade; CellGro®) and 100 ng/ml recombinant human granulocyte–macrophage colony-stimulating factor (GM-CSF) (GMP grade; Cell- Gro®) for 7 days. DC maturation was performed with various combinations of stimuli: TL, TL/TNF-α, or OK432 (Bicibanil, Chugai Pharmaceutical Co. Ltd, Tokyo, Japan) (Figure 1). Basic DC-preparation protocol comprised of TL and OK-432. Modified DC-preparation protocol comprised of TL, TNF-α and OK-432. On day 7, the generated DCs were

**Table 1.** Characteristics of study patients.

| No. | Gender | Age | Diagnosis | Metastatic tumor | Recurrence | primary | Protocol |
|---|---|---|---|---|---|---|---|
| 1 | M | 26 | Osteosarcoma | Lumbar, lung | + | Tibia | Basic |
| 2 | M | 15 | Osteosarcoma | Lung | + | Tibia | Basic |
| 3 | F | 9 | Osteosarcoma | Lung, lumbar | - | Femur | Basic |
| 4 | M | 31 | Chondrosarcoma | Lung | - | Tibia | Basic |
| 5 | F | 53 | Leiomyosarcoma | Lung | + | Inguen | Basic |
| 6 | F | 19 | Osteosarcoma | Lung | - | Femur | Basic |
| 7 | F | 17 | Osteosarcoma | Pelvis, humerus, lumbar, lung | - | Femur | Basic |
| 8 | F | 49 | Osteosarcoma | Lung, tibia, brain | - | Femur | Basic |
| 9 | F | 61 | Clear cell sarcoma | - | + | Foot | Basic |
| 10 | F | 40 | ASPS | Lung | - | Hand | Basic |
| 11 | M | 65 | Leiomyosarcoma | - | + | Thigh | Basic |
| 12 | M | 24 | Osteosarcoma | Lung | - | Femur | Basic |
| 13 | M | 45 | Osteosarcoma | Lung, femur | + | Pelvis | Basic |
| 14 | M | 19 | Osteosarcoma | Lung, brain | - | Femur | Basic |
| 15 | M | 59 | MFH | Lung | + | Tibia | Basic |
| 16 | M | 29 | Angiosarcoma | Lung | - | Lower leg | Basic |
| 17 | M | 43 | Chondrosarcoma | Lung, calcaneus | - | Tibia | Basic |
| 18 | F | 43 | Clear cell sarcoma | Lung | - | Lower leg | Basic |
| 19 | F | 26 | Clear cell sarcoma | Thigh, inguen | - | Lower leg | Basic |
| 20 | M | 59 | Synovial sarcoma | lung | - | Lower leg | Basic |
| 21 | M | 30 | Osteosarcoma | Lung | - | Femur | Basic |
| 22 | F | 39 | Chondrosarcoma | - | + | Pelvis | Modified |
| 23 | M | 37 | Liposarcoma | Lung | - | Thigh | Modified |
| 24 | F | 27 | Osteosarcoma | Lung | - | Pelvis | Modified |
| 25 | F | 41 | Synovial sarcoma | Lung | - | Back | Modified |
| 26 | F | 24 | Synovial sarcoma | Lung | - | Inguen | Modified |
| 27 | M | 64 | MFH | - | + | Back | Modified |
| 28 | F | 8 | Ewing's sarcoma | Lung | - | Calf | Modified |
| 29 | M | 31 | Osteosarcoma | Lung | - | Femur | Modified |
| 30 | F | 64 | MFH | Lung | - | Shoulder | Modified |
| 31 | F | 28 | Osteosarcoma | Lung | - | Pelvis | Modified |

Protocol: DC-preparation protocol; MFH, malignant fibrous histiocytom; ASPS, alveolar soft part sarcoma; MPNST, malignant peripheral nerve sheath tumor.
doi:10.1371/journal.pone.0052926.t001

**Table 2.** Comparison of %CD14$^-$HLA-DR$^+$ cells by DC maturation cocktails.

| Group | DC-preparation protocol | | %CD14$^-$HLA-DR$^+$ |
|---|---|---|---|
| Control | 1) | IL-4, GM-CSF | 45.4±2.5% |
| TL | 2),4) | IL-4, GM-CSF + TL | 50.0±1.8% |
| TNF-α | 5) | IL-4, GM-CSF + TL + TNF-α | 55.6±2.9%* |
| OK-432 | 3),6) | IL-4, GM-CSF + OK-432 | 60.1±1.9%** |
| | | Total | 52.5±1.2% |

CD14: mononuclear cell marker, HLA-DR: dendritic cell marker, IL-4: interleukin-4, GM-CSF: granulocyto-macrophage colony stimulating factor, TL: tumor lysate. Data±SEM *P<0.05, **P<0.01 versus control group.
doi:10.1371/journal.pone.0052926.t002

harvested and mixed for injection, and $5\times10^6$ cells were reconstituted in 1 ml normal saline. The DCs were injected in the inguinal or axillary region which the original tumor was closer. Treatment courses were performed every week and repeated 6 times. During the course of treatment, a portion of the cells were analyzed by flow cytometry to determine the degree of differentiation and maturation of the DCs.

## Flow Cytometry Analysis

DC preparation was assessed by staining with the following monoclonal antibodies: (MoAb) for 30 min on ice, antilineage cocktail 1 (lin-1; CD3, CD14, CD16, CD19, CD20 and CD56)-fluorescein isothiocyanate (FITC), anti-HLA-DR peridinin chlorophyll protein (PerCP) (L243), anti-CD14-allophycocyanin (APC) (MÖP9), anti-CD11c-APC (S-HCL-3), anti-CD123-phycoerythrin (PE) (9F5) (BD PharMingen, San Diego, CA, USA), anti-CD80-PE (MAB104), anti-CD83-PE (HB15a) and anti-CD86-PE (HA5.2B7)

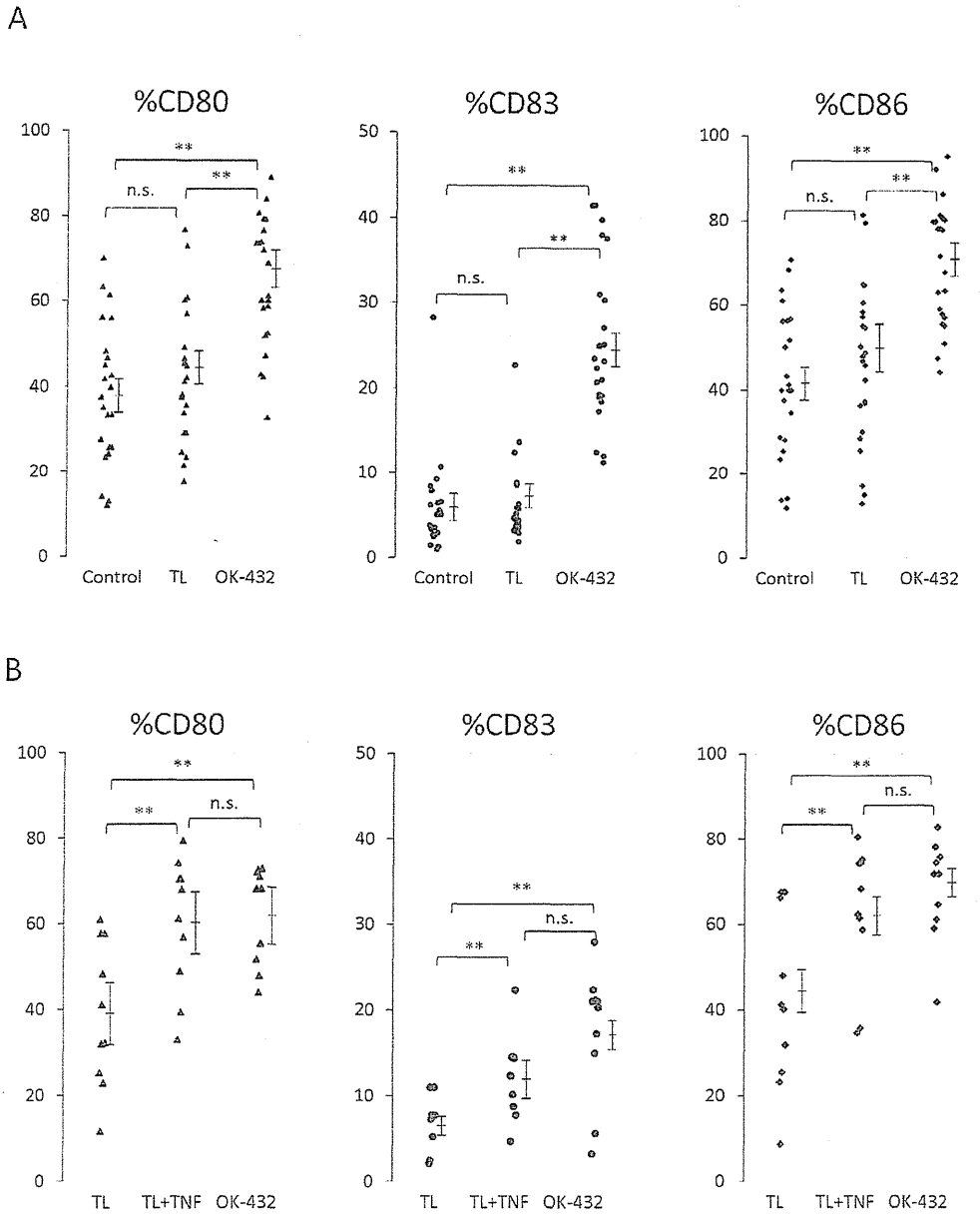


**Figure 2. Comparison of %CD80, %CD83, and %CD86 by DC maturation cocktails.** TL: tumor lysate, TNF: tumor necrosis factor-α, ** P<0.01, n.s.: not significant **A. Basic DC-preparation Protocol.** Cells treated with tumor lysate (TL) showed slightly higher maturation than control cells (not significant). Cells treated with OK-432 showed greater maturation (P<0.01). **B. Modified DC-preparation Protocol.** Cells treated with a combination of tumor lysate (TL) and TNF-α (TNF) showed markedly higher maturation than cells treated with TL (P<0.01).
doi:10.1371/journal.pone.0052926.g002

(Beckman Coulter, Fullerton, CA, USA). Cells were analyzed on a FACS Calibur™ flow cytometer. Data analysis was performed with CELLQuestTM software (Becton Dickinson, San Jose, CA, USA). To determine the degree of differentiation and maturation of DCs, %CD14$^-$HLA-DR$^+$, %CD80, %CD83, and %CD86 were measured.

## Immune Response

Blood samples were collected from patients before surgery and one and three months after surgery. IFN-γ and IL-12 were measured in order to determine the magnitude of the immune response following the DC-based immunotherapy.

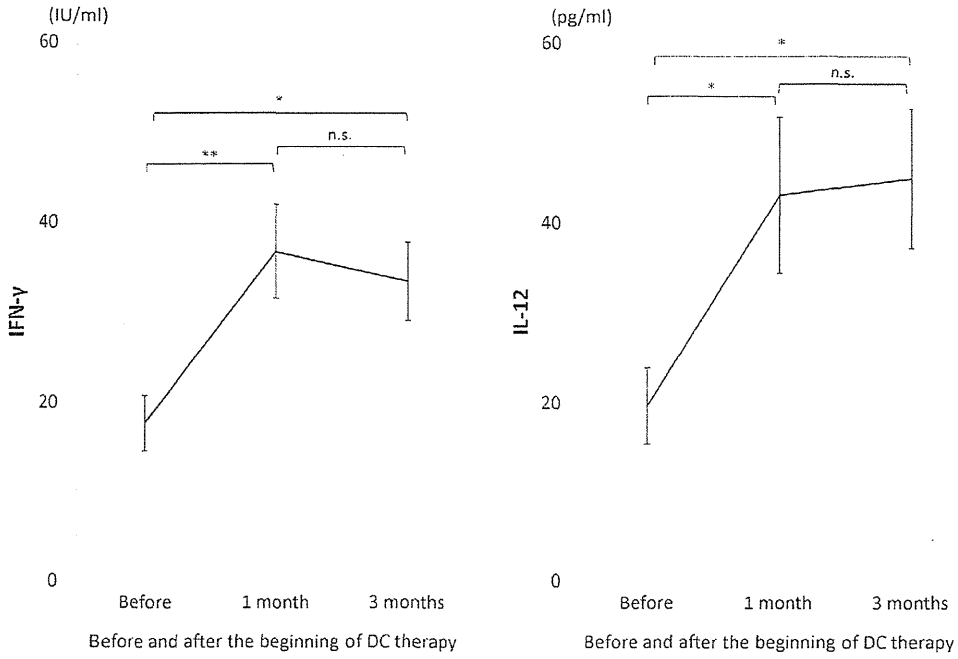


**Figure 3. Serum IFN-γ and serum IL-12 before and after DC therapy.** * P<0.05, ** P<0.01, n.s.: not significant.
doi:10.1371/journal.pone.0052926.g003

### Overall survival and progression free survival following the DC-based immunotherapy

Overall survival and progression free survival were evaluated by Kaplan-Meier method. Survival was defined as the time from the date of end of DC-based immunotherapy to the date of last follow-up or death due to any cause. Progression free was defined as the time from the date of end of DC-based immunotherapy to the date of last follow-up or tumor progression.

### Statistical Analysis

Results are expressed as mean ± SEM. Data were analyzed using one-way analysis of variance (ANOVA) test. Any P-values less than 0.05 were considered statistically significant. Statistical analyses were performed on a personal computer with the statistical package ystat2000 software.

## Results

### Patients

Thirty-one patients were included in this study. All the patients had metastatic and/or recurrent tumors. There were 14 males and 17 females, with a mean age of 36.3 years (8−64, Table 1). There were 16 patients with bone tumors (13 osteosarcoma and 3 chondrosarcoma,) and 15 patients with soft tissue tumors (3 clear cell sarcoma, 3 synovial sarcoma, 3 malignant fibrous histiocytoma (MFH), 2 leiomyosarcoma, 1 Ewing's sarcoma, 1 liposarcoma, 1

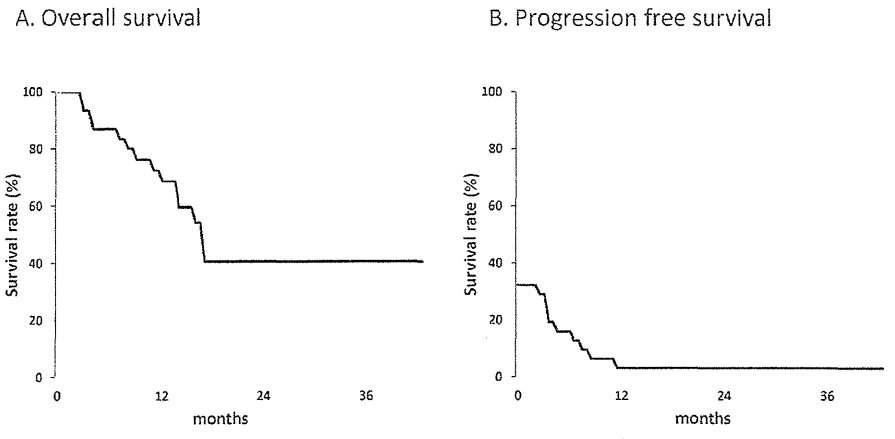


**Figure 4. Kaplan-Meier analysis of overall survival and progression free survival distributions for 31 patients with advanced malignant bone and soft tissue tumors.**
doi:10.1371/journal.pone.0052926.g004

alveolar soft part sarcoma (ASPS), and 1 angiosarcoma). None has experienced an adverse event during and after the treatment course.

### Differentiation of DCs

To determine the degree of differentiation, %$CD14^-HLA\text{-}DR^+$ was measured by flow cytometry. In total, 52.5±1.2% of cells were classified as $CD14^-HLA\text{-}DR^+$ cells (Table 2). The cells treated with IL-4, GM-CSF, and TL showed more differentiation than the cells treated with IL-4 and GM-CSF only (not significant). The cells treated with IL-4, GM-CSF, and OK-432 showed more differentiation than the cells treated with the other protocols ($P<0.01$). Furthermore, the cells treated with IL-4, GM-CSF, TL, and TNF-α showed more differentiation than the cells treated with IL-4, GM-CSF, and lysate alone ($P<0.05$). These results suggest that TL, TNF-α and OK-432 promoted the differentiation of DCs.

### Maturation of DCs

To determine the effects of DC maturation by TL, OK-432, and the combination of TL and TNF-α, %CD80, %CD83, and %CD86 were measured (Figure 2).

The effects of DC maturation by TL and OK-432 (basic DC preparation protocol) were analyzed (Figure 2–A). The %CD80 of the control group, TL group, and OK-432 group were 38.3±3.4, 42.4±3.2, and 64.2±3.1%, respectively. The %CD83 of the control group, TL group, and OK-432 group were 5.9±1.2, 6.2±1.0, and 25.1±1.9%, respectively. The %CD86 of the control group, TL group, and OK-432 group were 41.7±3.6, 45.5±3.9, and 69.9±3.0%, respectively. OK-432 group showed significant increase of %CD80, %CD83, %CD86 comparing with the other groups ($P<0.01$). However, there was no significant difference between TL group and control group. These results indicate that TL slightly induced the maturation of the DCs and that OK-432 markedly induced the maturation of DCs.

The effects of DC maturation by the combination of TL and TNF-α, or OK-432 (modified DC preparation protocol) were analyzed (Figure 2–B). The %CD80 of the TL group, TL + TNF-α (TNF) group, and OK-432 group were 39.1±5.3, 60.3±4.9, and 62.5±3.6%, respectively. The %CD83 of TL group, TL + TNF group, and OK-432 group were 4.5±1.1, 12.2±1.5, and 17.5±2.4%, respectively. The %CD86 of TL group, TL + TNF group, and OK-432 group were 42.0±6.5, 62.5±5.1, and 68.2±3.8%, respectively. Both of TL + TNF group and OK-432 group showed significant increase of %CD80, %CD83, %CD86 comparing with TL groups ($P<0.01$). These results indicate that the combination of TL and TNF-α markedly induced the maturation of DCs.

### Immune Responses

Serum IFN-γ and serum IL-12 were compared prior to DC-based immunotherapy, and one and three months after DC injection (Figure 3). Serum IFN-γ before DC injection, and one and three months after the injection was 17.6±3.1, 36.8±5.2, and 33.4±4.4 IU/ml, respectively. Serum IL-12 before DC injection, and one and three months after the injection was 19.7±4.3, 43.1±8.6, and 45.0±7.8 pg/ml, respectively. Both of IFN-γ and IL-12 showed significant increases after DC injection. These results indicate that our DC therapy induced the activation of immune responses one month after the therapy, and that the activated immune response is maintained for at least three months.

### Overall survival and Progression free survival

The mean follow-up of all patients was 14.9 months (range 2–43 months). Of the 31 patients, 17 patients were alive and 1 patient was progression free at the time of the final follow-up. Overall survival rates and progression free survival rates of the patients at 3 years were 68.7% and 3.2%, respectively (Figure 4).

## Discussion

The introduction of chemotherapy dramatically improved the treatment outcome for patients with primary bone and soft tissue sarcoma [21]. The standard surgery for bone and soft tissue sarcoma before the introduction of chemotherapy was limb amputation [21]. Consequently, the prognosis of patients with bone and soft tissue sarcoma was very poor before the introduction of chemotherapy. The most important prognostic factor before the introduction of chemotherapy was the metastatic lesions that existed before limb amputation. Unlike surgery and radiotherapy, chemotherapy shows systemic antitumor effects, which affect primary tumors and metastatic tumors. However, the continuation of chemotherapy causes many complications, such as renal failure, heart failure, and neuropathy. In cases with local recurrence or metastatic tumors, complications make it difficult to continue the chemotherapy course. Therefore, further systemic treatment of sarcoma is required an improved prognosis of patients with bone and soft tissue tumors. Recently, many experimental and clinical studies concerning immunotherapy for the treatment of malignant tumors have been reported [12]. Additionally, some patients showed a possible tumor suppressive effect of immunotherapy, indicating that this could be a promising approach in the treatment of patients with refractory malignant tumors.

Immunotherapy is classified as either non-specific immunotherapy or tumor specific immunotherapy [22,23]. Non-specific immunotherapy includes cytokine therapy, lymphokine-activated killer cells therapy, natural killer cell therapy, ERM activated killer cell therapy, and CD3-activated T cell therapy. Tumor-specific immunotherapy includes DC-based immunotherapy, cytotoxic T lymphocyte therapy, and peptide-vaccine therapy.

DCs play a critical role in T cell priming, as well as direct and cross-priming [12]. In the steady state, nonactivated (immature) DCs present self-antigens to T cells, which leads to tolerance through different mechanisms. Once activated (mature), antigen-loaded DCs promote T cell proliferation and differentiation into helper and effector cells. DCs are also important in launching humoral immunity. This is partly due to their capacity to directly interact with B cells and to present unprocessed antigens. DCs demonstrate tumor-specific antitumor effects by presenting tumor-specific antigens to immune cells. Furthermore, DCs play a pivotal role in the immunity to tumors. Once a dendritic cell takes up tumor antigens, the dendritic cell will present the tumor antigens to 100– 5,000 lymphocytes. Therefore, DC-based immunotherapy seems to be an efficient treatment for malignant tumors. However, the population of DCs in PBMCs is 0.2% [24], which is too low to make their collection practical for clinical applications [15]. Methods of collection or generation of DCs are required in order to use DC-based immunotherapy clinically. To date, PBMCs-derived DCs have been commonly used for DC-based immunotherapy.

IL-4 and GM-CSF are commonly used for the differentiation of DCs. Nakamoto et al. [25] reported that 45% of PBMCs in patients with hepatocellular carcinoma were differentiated into DCs by the treatment with IL-4 and GM-CSF. This study showed that 52.5% of PBMCs in patients with bone and soft tissue tumors were differentiated into DCs by IL-4 and GM-CSF. Furthermore,

DC maturation requires stimuli such as IL-1β, TNF-α, IL-6, or prostaglandin $E_2$. Although various DC maturation cocktails have been reported, there is no gold standard method for DC maturation for DC-based immunotherapy. OK-432 (Picibanil), a penicillin-killed Streptococcus pyogenes, is reported to have potent immunomodulation properties in cancer treatment [26]. Hovden reported that OK-432 induces the maturation and migration of DCs and stimulates the secretion of Th-1 type cytokines [27]. Our results show that OK-432 had a strong effect on DCs-differentiation and DC maturation. Although OK-432 has strong effects on DC-differentiation and DC maturation, OK-432-pulsed DCs are not able to activate tumor antigen-specific immunity. Conversely, tumor antigen-pulsed DCs can induce a tumor-specific immune response. Hsu *et al.* [10] reported that DC pulsed with a tumor antigen could elicit specific tumor-reactive T cells, and have clinical efficacy in patients with lymphoma. As with other malignancies, TL-pulsed DCs seem to be effective in the treatment of sarcoma. Our results showed that the TL slightly promoted differentiation and maturation of DCs. The effect of promoting DC-differentiation and DC maturation suggests the existence of tumor-specific antigens in many malignant bone and soft tissue tumors. Additionally, our results showed that TNF-α has a strong effect on promoting DC maturation. The TL/TNF-α pulsed DCs showed 1.6– 1.7 times greater maturation than the TL-pulsed DCs. Although TL-pulsed DCs can present tumor antigens, the TL-pulsed DCs showed only slight maturation. TNF-α promotes the maturation of TL-pulsed DCs. The well-differentiated and well-matured DCs generated by our DCs-generation protocols are considered to have strong tumor antigen-specific effects.

DC-based immunotherapy has been generally ineffective in promoting tumor rejection. The failure may be attributed to the use of insufficiency matured or activated DCs. In patients with advanced and metastatic cancer, immunity is generally suppressed by factors produced by tumors and tumor infiltrating cells such as regulatory T cells [28]. In order to overcome the immunosuppressive circumstances around tumors, inductions of sufficiently activated DCs, which highly express MHC molecules, CD80, CD86, and IL-12, are required. The existence of matured DCs around tumors has a great importance in antitumor immune response and prognostic significance [29,30]. Ménard et al. reported that levels of IFN-γ significantly correlate with progression-free survival [31].

Therefore, evaluations of the DCs-maturation and DCs-related cytokines are important in the DC-based immunotherapy. In this study, levels of IFN-γ and IL-12 were measured before and after the immunotherapy. The immunological responses are commonly evaluated by IL-12 and IFN-γ because these cytokines reflect the activation of the DCs [14,32–35]. Furthermore, it is reported that the existence of tumors does not influence the levels of the serum IL-12 and IFN-γ [32]. IL-12 secreted by DCs acts on IFN-γ production by Th1 cells. IFN-γ activates natural killer (NK) cells and cytotoxic T lymphocytes (CTL) that contribute to optimal antitumor immunity. Although chemotherapy shows rapid effects on tumors, DC-based immunotherapy shows slow tumor regression. The immune response is highest at 8– 10 weeks after DC-injection [36]. This study showed significant elevations of IFN-γ and IL-12 at one and three months after DC-based immunotherapy. However, a limitation of this study is the lack of data about serum IFN-γ and IL-12 in placebo group. Therefore, it seems that tumor progression influenced the increase of serum IFN-γ and IL-12. There are some reports about the correlation between tumor progression and serum cytokine levels [37,38]. Tsuboi et al. [37] reported that mean serum IL-12 level in patients with esophageal carcinoma (n = 70) was significantly higher than that in healthy volunteers (15). The levels of serum IL-12 correlated with tumor growth and progression, although the there was no significant correlation between serum IL-12 level and tumor progression. Morreti et al. [38] reported the difference of the serum IL-12 and IFN-γ levels in control population (n = 45), patients with localized melanoma (n = 11), and patients with metastatic melanomas (n = 34). Mean serum IL-12 level of the patients with localized melanomas was lower than that of the patients with metastatic melanomas. Mean serum IFN-γ level of patients with localized melanoma was higher than that of patients with metastatic melanomas, although there is no significant difference. In our study, serum IL-12 and IFN-γ showed significant increases which are much higher than the influence of tumor progression. These results suggest that the increase of the serum IL-12 and IFN-γ levels were influenced by the DC-based immunotherapy.

## Conclusions

DCs-based immunotherapy is a promising approach for the treatment of malignant tumors. In this study, about 50% of PBMCs were differentiated into DCs, and markedly matured by the combination of GM-CSF, IL-4, TL and TNF-α. Our results contribute to the development of DC-based immunotherapy for malignant bone and soft tissue tumors.

## Acknowledgments

The authors greatly appreciate Youko Kasai for technical assistance.

## Author Contributions

Conceived and designed the experiments: SM HN AT HT. Performed the experiments: SM HN YT MT. Analyzed the data: SM HN. Contributed reagents/materials/analysis tools: NY TS KH HK KI EM YN SK HT. Wrote the paper: SM HN HT.

## References

1. Banchereau J, Briere F, Caux C, Davoust J, Lebecque S, et al. (2000) Immunobiology of dendritic cells. Annu Rev Immunol 18: 767–811.
2. Palucka K, Banchereau J (1999) Dendritic cells: a link between innate and adaptive immunity. J Clin Immunol 19: 12–25.
3. Pulendran B, Banchereau J, Maraskovsky E, Maliszewski C (2001) Modulating the immune response with dendritic cells and their growth factors. Trends Immunol 22: 41–47.
4. Gregoire M, Ligeza-Poisson C, Juge-Morineau N, Spisek R (2003) Anticancer therapy using dendritic cells and apoptotic tumour cells: pre-clinical data in human mesothelioma and acute myeloid leukaemia. Vaccine 21: 791–794.
5. Villadangos JA, Schnorrer P, Wilson NS (2005) Control of MHC class II antigen presentation in dendritic cells: a balance between creative and destructive forces. Immunol Rev 207: 191–205.
6. Figdor CG, de Vries IJ, Lesterhuis WJ, Melief CJ (2004) Dendritic cell immunotherapy: mapping the way. Nat Med 10: 475–480.
7. Bayry J, Lacroix-Desmazes S, Kazatchkine MD, Hermine O, Tough DF, et al. (2005) Modulation of dendritic cell maturation and function by B lymphocytes. J Immunol 175: 15–20.
8. Crittenden MR, Thanarajasingam U, Vile RG, Gough MJ (2005) Intratumoral immunotherapy: using the tumour against itself. Immunology 114: 11–22.
9. Sanchez-Sanchez N, Riol-Blanco L, Rodriguez-Fernandez JL (2006) The multiple personalities of the chemokine receptor CCR7 in dendritic cells. J Immunol 176: 5153–5159.
10. Hsu FJ, Benike C, Fagnoni F, Liles TM, Czerwinski D, et al. (1996) Vaccination of patients with B-cell lymphoma using autologous antigen-pulsed dendritic cells. Nat Med 2: 52–58.
11. Nestle FO, Alijagic S, Gilliet M, Sun Y, Grabbe S, et al (1998) Vaccination of melanoma patients with peptide- or tumor lysate-pulsed dendritic cells. Nat Med 4: 328–332.
12. Steinman RM, Banchereau J (2007) Taking dendritic cells into medicine. Nature 449: 419–426.